Applying ADCPs for long term monitoring of SSC in rivers

Rui Aleixo[1], Massimo Guerrero[1], Michael Nones[2], Nils Ruther[3]

[1]University of Bologna, Department of Civil, Chemical, Environmental and Materials Engineering, Via Terracini, 28, 40131 Bologna, Italy

[2]Institute of Geophysics - Polish Academy of Sciences, Hydrology and Hydrodynamics Department, Ksiecia Janusza 64, 01-452 Warsaw, Poland

[3]NTNU Department of Civil And Environmental Engineering, Vassbygget, 405, Valgrinda, S. P. Andersens veg 5 Trondheim, Norway

Key Points:

- Long term suspended sediment transport monitoring with a novel acoustic method validated with direct samples in two different case studies
- Characterization of inorganic and organic fractions in suspended sediment transport
- Flow discharge to suspended sediment concentration curves and hysteresis analysis through hydrological events

Corresponding author: Rui Aleixo, rui.aleixo@unibo.it

This article has been accepted for publication and undergone full peer review but has not been through the copyediting, typesetting, pagination and proofreading process which may lead to differences between this version and the Version of Record. Please cite this article as doi: 10.1029/2019WR026087

Abstract

The flow rate and the suspended sediment concentration (SSC) of two different rivers draining into the Adriatic Sea basin, the Secchia in Italy and the Devoll in Albania, were analysed by processing the data collected in a 245-days period at monitoring stations equipped with side-looking acoustic Doppler current profilers (H-ADCPs).

SSC was determined as a by-product of the echo profiles along the horizontal aligned acoustic beams emitted by H-ADCPs. For the first time, the effect of organic matter other than a change of inorganic particles size distribution was evaluated as a possible reason for backscatter and attenuation variations during hydrological events. This reduced average deviations between acoustically inferred and sampled concentrations from one order of magnitude to 20% of actual values. The improvement required the measuring of attenuation to backscatter ratio (ABR) in addition to sound attenuation. The validation interval covered three order of magnitudes from $10^{-1}\,\mathrm{gl}^{-1}$ to $10\,\mathrm{gl}^{-1}$.

In this paper the potential of the ABR-method using H-ADCP to continuously monitor suspended sediment fluxes is tested in two different rivers, enabling single peak flood analysis and reliable assessment of sediment budget across a river cross-section. The advantages and disadvantages of this method are presented and discussed.

1 Introduction

The evaluation of sediment fluxes is paramount for a variety of environmental and engineering practices which include inland navigation (Paarlberg et al., 2015), erosion hazard mitigation during flood (Elhakeem et al., 2017), irrigation water supply, habitat and river morphology preservation (Guerrero et al., 2015; Haimann et al., 2016; Nones & Gerstgraser, 2016), and environmental sustainable hydropower development (Felix et al., 2016).

The prediction of sediment concentration is still a challenging problem in river hydraulics because universal and univocal relationships between flow discharge and sediment concentration, which depends also from the watershed supplying of sediment through precipitation, do not exist. Therefore, the use of functional relations between flow discharge and sediment concentration (i.e., sediment rating curves) has to be frequently calibrated through seasons and years to eventually account for climate variations, which might trigger different portions of the drainage basin in different periods (Horowitz, 2003;

Rainato et al., 2018; Comiti et al., 2019). This uncoupling between stream flow and sediment concentration is even more relevant in the case of very fine inorganic particles and organic matter, which are transported fully suspended in the water column up to far downstream from the origin area of supply. In this case, wash-load usually refers to suspended matter (organic and inorganic) not interacting with river channel bed whereas the suspended load is intended as inorganic sediment taken into full suspension from the riverbed. Although a clear separation between these two modes of transport is only for sake of theoretical classification, hereafter suspended sediment concentration (SSC) refers to the total concentration of suspended matter (organic and inorganic).

The heterogeneity of watershed and precipitation events reflect in the organic-inorganic quality and particle size distribution (PSD) of suspended sediment. This may result in very different SSC for the same stream power, in fact, finer sizes to be set in suspension require a lower stream power for a given SSC, for example. Frequent sampling should then be conducted to eventually establish stream flow to SSC rating curves valid for specific periods and active portions of the watershed. Unfortunately the direct sampling of SSC by means of traditional methods (i.e., physical samplers) is a challenging task especially during high discharges and turbulent water-level conditions in a river. This is particularly relevant in the case of mountain streams, where water velocity can reach significant values ($> 2 \mathrm{ms}^{-1}$) during floods making measuring challenging by means of traditional sediment samplers. In addition, the continuous monitoring of SSC in a fixed position is hardly achievable by means of direct sampling because of the time and effort required for field operations and subsequent laboratory analyses. To overcome this, in the last years, a variety of indirect methods have been developed, where light and sound scattering and attenuation were used as a surrogate measurement of SSC (Agrawal & Hanes, 2015; Guerrero et al., 2017).

SSC monitoring stations are usually based in optical turbidity meters however, more recently, the acoustic Doppler current profiler (ADCP) has become an extremely popular device for SSC assessment in rivers (Wright et al., 2010; Sassi et al., 2012; Moore et al., 2012; Guerrero et al., 2013; Venditti et al., 2016; Szupiany et al., 2019). This success was mainly due to the fact that the echoes profiling into the water column is a by-product of flow discharge measurement by an ADCP. The echoes profiles analysis eventually gives the SSC in addition to flow discharge. These hydraulics parameters combine into the suspended sediment flux. Particularly relevant the effort produced by the agen-

cies, such as the United States Geological Survey (USGS), for which the producing of reliable dataset about sediment fluxes is paramount for environmental protection and civil engineering applications.

This paper aims to apply a method based on the echo profile measured by an H-ADCP to continuously monitor the SSC in two very different rivers. The aplication of this method is tested to study single hydrological events. Furthermore, the effect of organic and inorganic matter in the SSC results is also analyzed.

1.1 State of the art

Empirical and semi-empirical methods were proposed to relate the SSC with acoustic backscatter. In fact, the ADCP is a monostatic, coherent acoustic device which emits and receives ultrasound pulses by mean of a number of transducers (at least three for flow velocity assessment). This means that, following the emission from the transducers, the emitted pulses travel along acoustic beams up to targets (i.e., suspended particles) which reflect sound back to the same transducers. The observation time is subdivided into gates such as targets at different distances from transducers reflect sound back (namely, backscatter) at different times, this originates echoes profiles.

The backscatter at gates and the cumulated sound attenuation along the profile were related to target features which are the SSC and PSD. This entails the inversion of the sonar equation which is herein reported in a simplified form in decibel (Guerrero & DiFederico, 2018). This straightforward relates the measured intensity level of echoes along the gated beam (i.e., the ranging distance r), $I_{\mathrm{dB}}(r)$, in the left hand term to the target features (i.e., SSC and PSD) which are embedded in the right hand term. In fact, the sound attenuation, α_s, and the backscatter, σ_s^2, in eq. (1) depend on suspended sediment concentration and particle size distribution.

$$I_{\mathrm{dB}}(r) - K + 20\log(r\psi) + 40r\log(e)\,\alpha_w = -40r\log(e)\,\alpha_s + 10\log\left(\sigma_s^2\right) \tag{1}$$

The other parameters in eq. (1) are the near field correction, ψ, and the sound attenuation due to clear water α_w, which do not depend on SSC and PSD and are therefore usually assessed under models provided in the acoustical oceanography and under-

water acoustics literature (Kinsler et al., 2000). Finally, K summarizes the instrumental parameters that fix the emitted energy.

A number of ADCP users (e.g. Wright et al. (2010); Moore et al. (2012); Guerrero and DiFederico (2018)) have produced multiple efforts to calibrate eq. (1). In fact, the ADCP is a commercial device and the echo profiling a by-product for which the manufacturers don't usually provide the instrumental parameters needed in eq. (1). Furthermore, eq. (1) is valid for averages quantities among pulses ensemble and within the acoustic sampling (namely, the ensonified volume) resulting in additional uncertainty. In addition to these technical limitations, the actual PSD in the ensonified water volume is not trivially related to α_s and σ_s^2. These occurrences led to a variety of case study driven approaches.

These approaches rely on specific assumptions to enable the inversion of the sonar equation and eventually assess the SSC. Most advanced methods additionally provide an estimation of the corresponding PSD parameters (e.g., the mean grain size of suspended sand is assessed in Guerrero et al. (2013)).

The discussion of these approaches is beyond the objective of the present work, however it is worth noting that semi-empirical methods using ADCPs were developed under Thorne and Hanes (2002) and Thorne and Meral (2008), which investigated the attenuation and scattering models for suspended mixture of inorganic particles also accounting of viscous attenuation due to fine particles (Urick, 1948; Flammer, 1962). These works mainly refer to small scale processes in inorganic sediment dominated environments (e.g., breaking waves at sea shore), for which specific acoustic devices were developed which relaxed some of the encountered challenges by ADCP users (e.g. instrumental parameters unknown, scattering variability within large volumes). Unfortunately, these devices are not suited to large-scale environment such as fluvial applications. In addition, the ADCP provides the flow discharge, which is a paramount parameter for sediment flux assessment too, although the mentioned disadvantage for SSC estimation. Other than these technological issues, the acoustic methods proposed so far for SSC evaluation in rivers by means of ADCP don't consider organic matter, whereas relevant efforts were produced to account for PSD change. For example: (i) Wright et al. (2010) discriminated silt-clay concentration from suspended sand using H-ADCP with horizontal aligned beams; (ii) Moore et al. (2012) used H-ADCP for the monitoring of SSC during flood also sug-

gesting multi-frequency approach (i.e., an array of H-ADCP working at different frequencies) to eventually account for PSD change during flood; (iii) Guerrero et al. (2013) used two ADCPs working at different frequencies on the same water column to provide profiles of SSC and corresponding mean diameter of suspended sand from the riverbed; (iv) Szupiany et al. (2019), estimated sand concentrations using ADCP by empirically decoupling the attenuation effect due to clay-silt concentration. All those methods considered the inorganic particles as the only reason for scattering and attenuation. Indeed, eq. (1) appears as an oversimplification of the sound propagation process in a water volume. Previous research efforts focused on different terms of that equation (e.g., α_s and σ_s^2 relation to clay-silt and sand concentrations, respectively) but fully neglecting the organic matter effectiveness on sound propagation.

In the results presented herein a noticeable effect appears on sound attenuation and backscatter, which was clearly related to the observed concentration of organic matter. Therefore, this study aims at demonstrating the need of accounting for suspended matter quality (i.e., organic and inorganic) change into the sonar equation in addition to inorganic particles size distribution change. These variations are particularly relevant for the long term monitoring of SSC and sediment fluxes through hydrological events, seasons and years. To address this issue, this study, starting from the usual sonar equation as reported in eq. (1), proposes a simplified approach to account for PSD change that is based on the measuring of attenuation to backscatter ratio, i.e., the ABR-method, already presented in (Guerrero & DiFederico, 2018). They demonstrated that the ABR does not depend on SSC but is straightforward related to PSD of inorganic matter for a wide range of variation in the PSD first and second orders momentum (i.e., mean and standard deviation). The PSD fixes the instrumental sensitivity to the attenuation produced by SSC. The instrumental sensitivity variation is estimated by means of a conversion function between ABR and the sound attenuation for unit SSC (i.e., the normalized attenuation) that depends on the actual PSD. This is valid for sound propagation into a homogeneous concentration of water-sediment mixture, which is the assumption made by Moore et al. (2012) in their attenuation method for the monitoring of SSC during flood by means of a single frequency H-ADCP. Therefore, the ABR-method using H-ADCP was herein applied for the first time in the field to account for PSD change, eventually obtaining a continuous and reliable monitoring of SSC by means of the attenuation method. In this way flow discharge and SSC were provided at the same time

across two different river channels, even for changing PSD throughout hydrological events and seasons which may affect instrumental sensitivity to actual SSC. Once the H-ADCP is firmly fixed in a river bank and the continuous communication with a remote server enabled, this technique has proven to be quite robust, being able to measure even during challenging conditions.

1.2 Work layout

The conversion relation between ABR and instrument sensitivity was validated in two rivers draining into the Adriatic Sea: the Secchia River, an Apennine tributary of the Po River in Italy, that flows into the north Adriatic, and the Devoll in Albania, which confluences in the Seman River and outflowing in the Ionic part of the Adriatic-Mediterranean Sea. These represented very different case studies in terms of morphological and hydraulics features: the Devoll River is a mountain wild stream whereas the Secchia River is a lowland regulated channel. The proposed methodology performed well in both cases which demonstrate the flexibility of the presented approach. Furthermore, the Secchia is a fully gauged basin by the Regional Agency for Prevention, Environment and Energy of Emilia-Romagna (ARPAE), which provided additional SSC data for a comparison with H-ADCP results. The conversion relationships among ABR and instrument sensitivity were validated by means of results from direct samples from both rivers. A larger effort was conducted at the Albanian case study, located in a remote area where no hydrological services are present. Water samples were collected from both rivers. These samples were filtered, and the filtered matter was analysed in terms of organic and inorganic composition. This bore out an effect of suspended organic matter in addition to PSD influence on ABR as proposed by (Guerrero & DiFederico, 2018) and empirically demonstrated the need to account for suspended matter quality into eq. (1).

The proposed H-ADCP methodology enabled the continuous monitoring of flow discharge and suspended sediment concentration for 245 days comprised between 2017/11/07-2018/07/10 at the two rivers. The continuous monitoring performed in the Secchia River through hydrological events in November and December 2017 was compared to the corresponding monthly estimations made available by the ARPAE at the time of this manuscript preparation, which are based on infrequent sampling of SSC. This demonstrated the need of continuous monitoring for a reliable estimation of sediment budgets flowing across the equipped cross-section.

Finally, the obtained relationships among flow discharge, SSC and ABR, made evident different hydro-sedimentological processes producing and advecting sediments up to the river channel cross-sections where H-ADCP were deployed.

Summarizing: to the authors' best knowledge, this is the first time that the ABR-method is applied in the field. This provided complete and detailed datasets of the suspended matter quality and concentration variation throughout hydrological events and in two different rivers by using H-ADCPs. Furthermore, an indirect acoustic method based on eq. (1) is discussed and tested on the basis of evidences regarding suspended matter quality other than inorganic particle sizes distribution. Finally, the unreliability of SSC infrequent sampling is put into evidence for the assessment of cumulated sediment budget through a river channel cross-section, and more generally speaking the lack of correlation between flow discharge and SSC.

2 Methods and materials

2.1 The acoustic method

Recalling eq. (1), on the right-hand side, the sediments attenuation coefficient, $\alpha_s = \zeta_s C$, and the backscatter, $\sigma_s^2 = k_s^2 C$, both depend on the suspended sediment concentration, C, and the PSD through the normalized attenuation coefficient, ζ_s, and the backscatter strength coefficient, k_s^2, respectively. ζ_s describes the viscous and scattering attenuation of sound due to sediment particles suspended in a viscous fluid. The viscous dissipation is due to shear produced by the relative motions of particles and the fluid that is relevant for clay and silt fine particles (Urick, 1948; Flammer, 1962). The scattering of incident waves out of the incident beam does not contribute to backscatter but it is lost energy. This was accounted for in the scattering attenuation. Backscatter and scattering attenuation prevail for coarse particles, i.e., sand, as described by (Thorne & Meral, 2008).

In the left-hand side one finds the known (e.g. clear water attenuation, α_w) and measured terms (e.g. I_{dB}), and in the right-hand side one finds two unknowns, related with the suspended matter attenuation and backscatter, namely α_s and σ_s^2, respectively.

In case of negligible gradient of SSC along the acoustic beam, eq. (1) can be interpreted as a linear fit equation, $y = mr + b$, along the ranging distance, r, where y stands for the known and measured terms, m, the slope, relates with the attenuation,

and the coordinate at the origin, b, with the backscatter. Differentiating equation(1) with respect to the ranging distance, r:

$$\alpha_s = \zeta_s C = -\alpha_w - \frac{1}{2r} - \frac{1}{40\log(e)}\frac{dI_{\mathrm{dB}}}{dr} \tag{2}$$

This is reasonably assumed from H-ADCP profiling (Moore et al., 2012), where the horizontally aligned beams intercept water volumes close to the same distance from riverbed. Eq. (2) shows that the attenuation can be obtained from the echo intensity slope. However, passing from this slope to SSC (i.e., C in eq. 2) also requires an estimation of the normalized attenuation coefficient ζ_s, which theoretically depends on PSD of suspended sediment. In previous H-ADCP applications, this was assumed to be constant in time. However, this assumption is not realistic for long-term monitoring of SSC in rivers. Aiming to overcome this limitation, relationships were here proposed among ABR and ζ_s. As a matter of fact the ABR is given by:

$$\mathrm{ABR} = \frac{\zeta_s C}{10^{\frac{10\log(k_s^2 C)}{10}}} = \frac{\zeta_s C}{k_s^2 C} = \frac{\zeta_s}{k_s^2} \tag{3}$$

which is independent of the sediment concentration. However, the ABR at a given frequency and for homogeneous concentration depends on the actual PSD and can be estimated from echo profiling (Guerrero et al., 2016; Guerrero & DiFederico, 2018). A non-trivial relation exists between PSD features (i.e., diameter, d; standard-deviation, std; and skewness, skw) and the ABR, so that a limited region for $d - std$ values may be associated to a known ABR at a given frequency. Furthermore, the normalized attenuation coefficient, ζ_s, depends on PSD features. Therefore, the measuring of ABR may lead to a likely range of $d-std$ values, which in turn may be used to estimate the normalized attenuation coefficient, ζ_s. The attenuation can thus be converted in sediment concentration by means of equation (2) as suggested by Moore et al. (2012).

$$C = \frac{1}{\zeta_s}\left(-\alpha_w - \frac{1}{2r} - \frac{1}{40\log(e)}\frac{dI_{\mathrm{dB}}}{dr}\right) \tag{4}$$

A key point of this method is the need to obtain meaningful relationships between ABR and the normalized attenuation coefficient ζ_s to eventually invert the sonar equa-

tion as reported in eq. (2). This entails a field validation by collecting water samples from the river simultaneously with echo measurements.

2.2 The application of the acoustic method

To better understand the application of the presented method, its main six steps are here described in detail. Figure 1 (a) depicts a flowchart with the sequence of operations to carry for computing the SSC.

In Step 1, two minutes averaged profiles (namely, ensembles) are acquired. This is an average of about 60 to 120 instantaneous profiles, measured by the H-ADCP at 0.5 Hz -1 Hz frequency, which depends on the actual ranging distance and the pulse length. After, each ensemble must be validated (Step 2). The validation includes the following operations:

1. Time-averaging: The median of blocks of 30 echo-profiles ensembles is taken to obtain hourly estimates. This minimizes random errors due to possible uneven performance of transducers and the electronic components, as well as spikes due to debris backscatter.
2. Background noise removal: subtracting the noise level that was the minimum echo intensity level along each profile.
3. Trimming the echo averaged profiles to water volume scattering, which excluded reflections from boundaries (e.g., the beam reflection from the opposite bank, Figure 1 (b), or the beam reflection below the water surface).

A final check was confirming if the number of points in the profile was enough to compute its derivatives (minimum of 3 points). No SSC data was computed in the case of too low water levels, which made the H-ADCP too close to water surface and the acoustic beams impacting the water surface from below at a distance within the blanking distance and the first cell. Furthermore, it was observed that, generally, it was not possible to compute the SSC for floods extreme peaks where the overall noise level due to turbulence and extremely sediment-laden fluxes limit the sound return to the first cell. These two limitations played different roles in the two case studies: the relative higher position of the H-ADCP at the Secchia enabled measuring extreme peaks but not during low water level periods, and the opposite for the Devoll case study.

In Step 3, the validated ensembles are linearly fitted with eq. (1) to determine σ^2 and α_s. This includes the modelling of clear water attenuation following Medwin and Clay (1998), accounting for measured pressure and temperature by ADCP auxiliary sensors. The instrumental parameter K accounted of voltage variation (from reading in the raw data file). Furthermore, it was tentatively fixed to agree with k_s^2 as resulted from samples (Thorne & Meral, 2008), on average. In Step 4, the ABR is computed and fed to Step 5. Step 5 is crucial for the successful application of the method, since a suitable relationship between ABR and ζ_s has to be introduced. This can be made in two ways, namely:

1. Using a valid relationship for a range of PSDs of inorganic sediment, considering for example the variation of the mean grain size of a well sorted PSD (i.e., a range of mono-granular distributions) or a family of log-normal distributions with changing standard deviation and mean size (Guerrero & DiFederico, 2018).
2. Using a relationship derived from direct measurements of ABR and SSC from H-ADCP profiling and water sampling, respectively, which straightforwardly gives ζ_s (i.e., $\zeta_s = \alpha_s/C$) .

When possible, the latter should be used since it will embed within ζ_s additional reasons other than PSD distribution changes for a modification of the attenuation sensitivity to SSC. In this connection, the ABR-ζ_s relationship may be better referred as the sensitivity function to SSC. Figure 1 (c) illustrates the monogranular and empirical relationships. It has to be stressed that the empirical relationships are site-dependent. This means that using a relationship obtained from a river in a different one, will lead to erroneous results.

Finally, in Step 6 the SSC is computed by means of equation (4). Since the echo profiles are acquired and processed (steps from 1 to 5, which include ABR assessment) for each time step, it is possible to compute for each time-averaged echo profile the corresponding SSC, thus resulting in time resolved measurements of SSC.

2.3 Case studies

The rivers chosen for this study were the Secchia in Italy, and the Devoll in Albania. These two rivers were chosen because of their differences: while the monitored reach

of the Secchia River lies in the lowlands, the Devoll is a mountain river. The Secchia River has been monitored in terms of flow and sediment load since the 60's of last century, the Devoll has been mostly ungaged since the early 90's of last century, and data retrieved from the previous period is not properly documented.

The Secchia is a tributary of the Po River, discharging into the Adriatic Sea. As for the Devoll, from its confluence with the Osum River, they form the Seman River that also discharges into the Adriatic Sea. Figure 2 shows the map of Italy and Albania with the indication of the estuaries of both Po and Seman rivers. The sediments transported by these watercourses are important to assess the different dynamical and ecological processes taking place in the Adriatic Sea (Milliman et al., 2016).

The Secchia River originates in the Tusco-Emilian Apennines valley at 1357 m above sea level, and it is a right-hand tributary of the Po River at south of Mantova, stretching for around 172 km and covering an area of about $2292\,\mathrm{km}^2$. Its yearly hydrological regime alternates between the spring and autumn floods and the summer and winter dry periods. According to the data provided by the Regional Agency for Environment and Energy (ARPAE, 2017), the mean flow measured at the La Pioppa station (46 km upstream of the Secchia-Po confluence), for the period 2004-2016 was $Q = 25.8\,\mathrm{m}^3/\mathrm{s}$. At this location, the drainage basin is $1377\,\mathrm{km}^2$ and the average slope is $i = 0.0003$. According to ARPAE (2017) the sediment yield for the Secchia River was $0.2\times10^6\,\mathrm{m}^3\mathrm{year}^{-1}$.

The measurement section chosen was located in Ponte Motta, Cavezzo, Italy. This is a provincial road bridge located about 8.3 km upstream La Pioppa station. The map, and the measurement station are depicted in Figure 3.

The Devoll is a mountain stream flowing in 1 km wide alluvial valley with typical braided morphology. The water discharge ranges between $10\,\mathrm{m}^3\mathrm{s}^{-1}$ and $10^3\,\mathrm{m}^3\mathrm{s}^{-1}$ (order of magnitude). According to Almestad (2015), the mean flow rate measured at Kokel for a period of 36 years was $Q = 28.3\,\mathrm{m}^3\mathrm{s}^{-1}$ for a drainage basin of $1879\,\mathrm{km}^2$. At Kokel the river slope was estimated to be $i = 0.015$. Data reported in Sigurd (2017) indicates that the sediment yield is about $2.4\times10^6\,\mathrm{m}^3\mathrm{year}^{-1}$ for Devoll at Kokel, less than half at basin closure ($3140\,\mathrm{km}^2$).

The Kokel measuring station is located on the left bank of the Devoll River, near Gramsh city, Albania, as depicted in Figure 4. In Kokel, a passage between steep sides

keeps the entire flow within 30 m width section that was suitable to monitor the flow discharge. Flow velocity measurements carried at this section have shown cross-section mean velocities up to 4 ms^{-1} during floods.

Estimated flow discharges from H-ADCP profiling versus water level measurement are reported in Figures 3 (e) and 4 (e) for the Secchia and Devoll, respectively, together with the surveyed cross-sections. These cross-sections contain the instrumental axis which corresponds to the bisector of H-ADCP 40° spaced acoustic beams. The level of H-ADCP profiling is indicated which is 2.8 m and 0.8 m above the channel thalweg for the Secchia and Devoll, respectively. Flow discharge and suspended sediment concentration assessments were limited to water levels of 0.1 m above the aforementioned levels. This was due to the acoustic beam reflection from below the water surface which accounts for the beam opening angle, therefore imposing a limit on the acoustic beam path across the water channel.

2.4 Field campaigns for validation

Several field campaigns were made in order to collect samples of suspended and bed sediments in both Secchia and Devoll rivers (see Table A1). Ten campaings were made on the Devoll River and four on the Secchia River. Some samples were also collected from the riverbed that were analysed in terms of PSD by means of dry sieving for fractions coarser than 75 μm and by settling method for finer fractions (i.e., $1 - 75\,\mu$m). These laboratory analyses were conducted under standard procedures (Head, 2006).

To sample and extract the suspended sediment concentration, a variety of technologies were chosen as function of the hydrological condition and the access to the area during flood events. Direct sampling was particularly challenging during floods at the Devoll because of the very high water velocities in the narrow cross-section which frequently exceeded 4 ms^{-1}. In addition, the Kokel bridge can be reached by foot only, following a steep trail, making it difficult to access under bad weather conditions. These conditions limited the use of the isokinetic sampler P-72 by USGS, because of the actual possibility of keeping it stable in the streamflow. However, it was lowered from the Kokel bridge at different depths and positions across the river channel, in three campaigns characterized by low water levels (Table A1) that provided a number of samples not biased by sucking and shading effects.

An automatic sampler (6712 Portable Sampler by Teledyne ISCO) was integrated in the Kokel monitoring station at the Devoll River. Under the station control system, this was successfully activated for levels exceeding 2.8 m which performed non-isokinetic sampling at the left bank close to the ADCPs. At medium water levels, additional samples were collected from water surface by manually lowering a bottle with a dead weight, from the Kokel bridge in the centre of the streamflow.

Furthermore, the LISST-ABS by Sequoia Inc. was used at medium-high levels at the Devoll. The LISST-ABS is a backscatter sensor, which profiles the echo intensity at 8 MHz in a small range of 5-10 cm. These profiles were converted into concentration values by accounting for sound dissipation and spreading, and assuming a backscattering coefficient, k_s^2, as assessed from PSD of direct samples. It is worth noting that this probe was easy to be deployed from the Kokel bridge attached to a dead weight or by towing a small vessel across the channel. This enabled a more extensive investigation of SSC gradients at the channel cross-section, which was particularly relevant to check the assumption made about SSC homogeneity distribution. Summarizing, more than 25 water samples from Kokel were sampled that, combined with the LISST-ABS data, provided a solid dataset of suspended sediment concentration values and corresponding particle size distributions.

As for the Secchia River, the sampling was performed from the Ponte Motta bridge where the H-ADCP was installed. Repeated campaigns were conducted by lowering the "Watertrap" produced by Eijkelkamp Soil & Water. This is a small cylinder with a tail fin which underwater aligns to the current. The cylinder was lowered down to 2-3 m deep, and in 2-3 sections across the channel depending on the water level and to eventually cover the entire cross-section, concurrently profiled by the H-ADCP. The cylinder is opened at the two ends which allows the flux to pass through, at the desired depth letting a weight falling down along the hanging cable, a 1.25 l volume of water volume is trapped. This simple sampler, although not designed for actual isokinetic sampling, worked properly in the Secchia River where the water velocity and depth were limited to about 1 ms^{-1} and 7 m respectively. A total of 24 samples were collected in different hydrological conditions characterized with water levels ranging from 1.5 m to 8.3 m.

The collected water samples were analysed following a standard procedure defined by IRSA-CNR (2003). The sediment concentration in the sampler bottles was derived

by weighting the filters with and without sediments, as well as the water for deriving the total volume. After weighting the previously dried filters of 0.45, 0.65, 0.80 and 3 μm pore diameter, the water was filtered through the different filters using a filtration ramp, starting with the larger pore diameter to the smallest. In this process a vacuum pump is used to increase the filtering speed. The filtered water was collected, and the filters were dried and weighed. Further processing consisted in heating the filters up to a temperature of 180^o C for a period of 20 to 25 minutes in order to burn the organic matter. The final weight of the filters was measured thus resulting in the total inorganic matter. Following this procedure, the volume of water and mass of sediments both organic and inorganic was determined. With this procedure, the total suspended sediment concentration, the suspended organic matter concentration and the suspended inorganic matter concentration were determined.

As for the particle size distributions of sediment contained in the collected water samples, these were assessed by means of laser diffraction sizers namely: the LISST portable XR, manufactured by Sequoia Scientific, (Sequoia, 2018), and the Analysette 22 (Fritsch, 2016). More details about devices and analyses combinations at each spot and campaign can be found in the annex.

2.5 H-ADCP monitoring stations

Side looking ADCPs by Teledyne-RDI (i.e., H-ADCP Channel Master) were installed in the bridge first pier starting from the right embankment of the Secchia River at Ponte Motta, Italy, and in an existing rock pocket at the left bank of the Devoll at Kokel, Albania (Figures 3 (c) and (d) for the Secchia and 4 (c) and (d) for the Devoll). These ADCPs allow for the simultaneous measurement of the flow velocity profile and of the echo profiles along cross section at the local level of 2.8 and 0.8 m for the Secchia and the Devoll respectively, roughly corresponding to about 2 m of water depth in both cases.

The H-ADCP is a coherent acoustic devices projects and receive ultrasound bursts along two horizontally aligned beams which are 40° spaced. This enables the reconstruction of the horizontal projection of water velocity vector along the profiles. The H-ADCP is typically applied for flow discharge assessment across a river channel by using the index method (Levesque & Oberg, 2012). Together with the measurement of water level performed by the sensors within the H-ADCP, it is then possible to obtain the grading

curves $Q - h$ (Figures 3 (e) and 4 (e)). Herein the echo profiling along the first beam was further exploited to measure SSC by means of the ABR-method.

In Ponte Motta only one H-ADCP working at 0.6 MHz was installed (Figure 3), whereas in Kokel two H-ADCP were installed working at 0.6 MHz and 1.2 MHz (Figure 4). The lower frequency allows a deeper penetration of the acoustic beam, whereas a higher backscatter and a better profiling resolution was expected for the 1.2 MHz. Temperature, pressure sensors, as well as additional upward pointing acoustic beam are integrated in the H-ADCPs, allowing for the measurement of both water temperature and level respectively.

Integrated in the Kokel measurement station is also an ISCO-6712 sediment sampler by Teledyne-ISCO, installed on a platform at 6 m level to minimize the risks from being damaged due to flooding events. The acquisition-control system used in both the monitoring stations is the LISC (Logical Intelligent System Control) by Communication Technology srl, Italy. This system continuously collects H-ADCPs raw ensembles and operates the ISCO sampler based on the water level reading from ADCP. Instantaneous profiles were averaged into 2 minutes ensembles and then recorded. The LISC is remotely accessed via GSM network and measured data are transmitted to a server using the same network. It is therefore possible to access instruments settings and data 24h a day, 365 days a year.

In both case studies, power was provided by a solar panel coupled to a 24 V battery. The monitoring station at Kokel has been continuously operating since 2016, whereas the station at Ponte Motta worked during the 245 days period herein analysed. Both stations, in particular the one located at Kokel, have proved to be quite sturdy having resisted to some severe flood events and requiring only minor maintenance periods.

3 Results

3.1 Direct sampling results

The water samples from the Secchia River gave a total SSC ranging from 0.149 gl^{-1} to 0.622 gl^{-1} that depended on the water level during sampling campaigns. This changed within the range of 1.50 m to 8.30 m in the local system. These SSC were pretty homogeneous distributed across the channel and along the water depth. The observed gradient was characterized with maximum deviation of 20% from the samples mean value

that was during low flow condition; whereas no more than 5% deviations resulted from samples at high level condition. The number of PSDs from laser diffraction were characterized with mean size, standard deviation and non dimensional skewness changing within the ranges 2.9 μm to 3.1 μm, 2.7 μm to 3.5 μm and 7.0 to 7.5, respectively. The PSD based on particles volume rather than on corresponding number represented well sorted material with d_{50} in the range of 5 μm to 10 μm.

Sampling campaigns at Kokel covered water levels from 1.0 m to 3.7 m and the total SSC resulted from a minimum of 0.076 gl^{-1} to the maximum sampled value of 8.035 gl^{-1} during the falling limb of a flood hydrograph. During a single campaign (i.e., with constant hydrological conditions) the observed deviations of SSC among samples at different depth and section across the channel, were quite low. As a matter of fact, during high level conditions, the maximum deviation was of about 35% of the mean value. This reached 63% for low water level. Regarding the particle size distributions, the mean sizes of number distributions changed in the range of 2.9 μm to 3.7 μm among samples, the corresponding standard deviations were in the range of 3 μm to 5 μm and skewness ranged between 4 and 7. The volume PSDs represented well sorted material with d_{50} equal to 7 μm to 10 μm.

The measured values of d_{50} from Secchia and Devoll riverbed samples were 31 μm and 240 μm, respectively. Very different compositions at the bottom were observed in the two case studies: the Devoll riverbed is formed by poorly sorted sediment ranging from clay to cobble whereas the Secchia channel is mostly covered of silt.

The organic and inorganic contents from samples were also analysed which resulted in relevant correlations with the ABR from H-ADCP profiling during sampling periods. In detail, the acoustic parameters changed in function of the organic matter fraction as indicated in Figure 5.

The acoustic parameters obtained from sampled total concentration and corresponding attenuation and backscatter measurements by H-ADCP, were adimensionalized by the respective values of the same parameters corresponding to particle size distributions of inorganic portion from the same samples, which are herein indicated by the subscript PSD. In other words, the values indicated with the subscript ADCP, are from the procedure from which the conversion lines (i.e., empty marks in Figure 6) were obtained, meanwhile the PSD values corresponds to expected estimations for observed particle size

distributions (i.e., filled marks in Figure 6) as suggested by Guerrero and DiFederico (2018) corresponding to ζ_s and k_s^2 values assessed according to Thorne and Meral (2008) and Urick (1948).

The non-dimensional ABR is higher for the larger concentrations (Figure 5 (a)). For those same concentrations it is possible to see that the organic content is smaller, between 2% and 8%. At the measured concentration of 0.598 gl^{-1} the non-dimensional ABR resulted equal to almost unity, that is, the suspended particulate behaves, from the perspective of the ABR, as a inorganic particulate. Furthermore, for this case, the organic material percentage was determined to be around 10%. Considering both non-dimensional backscatter and attenuation individually (Figures 5 (b) and (c)), it is possible to see that both increase with decreasing total concentration, and that, for lower concentrations, the percentage of organic material is higher. From this analysis it seems that a significant amount of backscatter and attenuation can be due to the unavoidable presence of organic material. This increasing of backscatter and attenuation for organic material is in accordance with findings from laboratory tests, (Bux et al., 2019). These authors measured orders of magnitude increase of both backscatter and attenuation, for given wave number radius products, when passing from inorganic coarse particles such as spherical glasses, very fine irregular particles of barium sulphate and titanium dioxide to colloidal organic emulsions. These emulsions were characterized with a density close to water and individual particle size in the Rayleigh scattering range, i.e., the wave number radius product in the range $10^{-4} - 10^{0}$. Other than organic material, microbubbles may also effectively increase the backscatter and attenuation, although this appears unlikely at low flow condition (i.e., low sediment concentration) in absence of rough water surface when the mentioned deviations from expected values, according to Thorne and Meral (2008) and Urick (1948), were observed. The observed backscatter and attenuation eventually resulted in low ABR for increasing percentage of organic matter (i.e., the percentage of weight lost after burning the sample at 180 °C). This results in an increased sensitivity of the acoustic method for suspended sediment concentration assessment. As a matter of fact, a larger value of ζ_s, will result in larger variations of the measured attenuation, α_s, for small changes of the total concentration C, as stated in eq. (4).

3.2 Validation of the ABR-method for SSC assessment

The water samples collected during the field campaigns were identified by the time (day, hour, minute) of the sampling. This allowed measuring the SSC at those times and to correspond the SSC measurements with the acoustic data from the ADCP, namely the corresponding echo profiles. This procedure, applied to both rivers, allowed to obtain the the relationship to pass from ABR as measured from H-ADCP to ζ_s, namely the conversion function ABR-ζ_s.

Suspended sediment samples collected from both the Secchia (open triangles) and the Devoll (open circles), determined the empirical relation from measured ABR to the observed normalized attenuation coefficient ζ_s (Figure 6). These observed values are the ratio between SSC from samples and measured attenuation (i.e., $\zeta_s = \alpha_s/C$ as presented in eq. (2), and $\zeta_s = m/C$ as from I_{dB} profiles linear interpretation). For the Secchia, since a small variation was observed, a linear fit was used. As it can be seen the conversion curve ABR$-\zeta_s$ for the Devoll is a non-linear function. In this case, a fit given by the ratio of a 2^{nd} and 1^{st} order polynomials was adopted. These functions are essentially empirical and allow to take into consideration the local properties of each river. It is important to mention, that the acoustic method presented in section 2.1 is general and can be applied to different rivers. However, this conversion function accounts for suspended matter variations among floods events and seasons thus including the local specific information.

This widens the application of eq. (1) to possible organic matter suspended in the measurement volume. In fact, the using of these empirical relationships substitute those derived by Guerrero and DiFederico (2018) on the basis of the scattering and attenuation models proposed by Thorne and Meral (2008) and Urick (1948), which are valid for PSD of inorganic matter.

The ABR to ζ_s conversion functions from samples (Figure 6) were used to implement the ABR-method and acoustically evaluate the SSC. These evaluations were eventually compared to SSC from samples which straightforwardly validated the method as can be appreciated in Figure 7. The validation, overall, covers a three order of magnitudes interval from $0.05\,\mathrm{gl}^{-1}$ to $8\,\mathrm{gl}^{-1}$. The coefficient of determination among acoustically inferred and sampled concentrations resulted equal to 0.96 and the root mean squared

error $0.54\,\mathrm{g\,l^{-1}}$. The average and maximal deviations between actual and assessed concentrations are 20% and 90% of the corresponding actual values, respectively.

Furthermore, in the same figure, a significant improvement is visible of the proposed method with respect to the method that is based on acoustic attenuation measurement only. This would result in one order of magnitude as average deviations. This improvement is due to the tuning of ζ_s on the basis of measured ABR, whereas ζ_s is considered as a constant parameter in the attenuation method.

3.3 Validation of the homogeneous concentration hypothesis

The ABR-method herein proposed is an advancement of the attenuation method for SSC assessment using H-ADCP. Both methods rely on the assumption of homogeneous concentration along the acoustic beam axis, meaning, a negligible gradient of concentration along the echo profile. This entails relevant simplification regarding the sediment flux evaluation other than the inversion of the sonar equation for SSC assessment. In this case, the sediment flux can be straightforwardly estimated by multiplying flow discharge by the assessed SSC and by neglecting any gradient across the cross-section and along the water depth.

The proposed ABR-method aims at reducing large sources of uncertainties in sediment flux estimation when using data produced by the long term monitoring using H-ADCP. These sources of uncertainty stem from infrequent sampling and assuming a constant value in time of the normalized coefficient, ζ_s. In the Secchia River case-study an order of magnitude difference resulted for November 2017 sediment budget as estimated from ARPAE's infrequent sampling at Ponte Bachelllo, 10 km upstream of the case-study monitoring station (Table 1); while the SSC assessment at the Devoll bore out an order of magnitude error when neglecting ABR to ζ_s relation (Figure 7) in the attenuation method. When compared to those, the effect of observed SSC gradients during sampling campaigns was found to be negligible. Those campaigns also included repeated measurement of the SSC across the river channel and along the water depth that bore out almost homogeneous distribution with variations always lower than 63% (Table A1) and particularly irrelevant for high water levels (i.e., for high SSC during flood events).

An analysis of the effect of SSC variation on the estimated sound attenuation, α_s, is herein proposed. The derivate of equation (1), for a variable sediment concentration along the ranging distance results in:

$$\alpha_s - \frac{1}{4C}\frac{dC}{dr} = -\alpha_w - \frac{1}{2r} - \frac{1}{40\log(e)}\frac{dI_{dB}}{dr} \tag{5}$$

Where dC/dr is the derivative of the sediment concentration profile across the channel width. This may produce an overestimation of the assessed attenuation from H-ADCP profiles in case of decreasing concentration along the ranging distance. This term was of the order of 10^{-2} Neper m^{-1} in case of a maximum observed gradient of SSC and 10^{-3} Neper m^{-1} on average among the performed campaigns. These variations are negligible when compared to the corresponding attenuation values as assessed from H-ADCP profiles under the homogeneity assumption which ranged between 0.2 and 0.6 Neper m^{-1}. The observed variations result in a maximum of 5% uncertainty in the SSC value, therefore it is reasonable to assume the homogenous hypothesis.

Moreover, the variation of the PSD along the ranging distance may eventually result in a bias. This would be reflected by an additional term in the left-hand side of equation (5), which embeds the derivative of the backscattering coefficient, k_s^2. No evidence was observed regarding the PSD variation along the ranging distance. However, it is worth noting that a sensitive analysis on the applied method for α_s assessment, bore out almost unchangeable estimations when considering a reduced ranging distances to meet the homogeneity assumption within a smaller measurement volume. Therefore, the homogeneity assumption appears reasonable in the presented study.

3.4 SSC measurements in Secchia and Devoll rivers

The proposed acoustic method presented in section 2.1 was coded and implemented in a graphical user interface (Aleixo et al., 2019). This allowed to process all the acquired data for both rivers in an efficient way. One of the key advantages of the proposed acoustic method is the possibility of using time series of ADCP echoes measurements to determine a corresponding time series of SSC. This allows to continuously monitor the water courses not only in terms of flow rate and water level, but of SSC as well. This is clearly showed in Figure 8 which reports a two-month period, for both Secchia and Devoll rivers.

Combining the measured flow discharge with suspended sediment concentration eventually provided their relationships at the two rivers (Figure 9). Aiming to elucidate the effectiveness of suspended matter type (i.e. organic and inorganic) in modifying instrumental sensitivity throughout hydrological events, the measured ABR is reported as a proxy of suspended particles size distribution (Guerrero & DiFederico, 2018). This allows identifying different regions in terms of ABR representing concentration-flow discharge clusters, which reflect specific features of sediments in suspension and corresponding hydro-sedimentological processes.

Major differences can be observed among the two rivers in terms of maximum values for the observed suspended sediment concentrations: $3\,\mathrm{gl}^{-1}$ was rarely reached at the Secchia River (Figure 9 (a)), meanwhile a plateau at a level of around $10\,\mathrm{gl}^{-1}$ is visible in Figure 9 (b) for the Devoll River. This plateau is most likely due to the impossibility of measuring extreme hydrological peaks at the Albanian case study, as already pointed out for the flow discharge measurement.

The integration of flow discharge times the SSC gave reliable estimations of the sediment load passing across the river channel in November and December 2017. These can be compared to corresponding values derived from ARPAE estimations (Table 1), which are the mean SSC from infrequent samples times the mean discharge at each period.

The underestimation of sediment loads computed from ARPAE data can be explained by the infrequent nature of the ARPAE sampling. In November, only 4 days out of 30 had valid H-ADCP data. In these four days, three concentration peaks were found. In December, about 16 days out of 31 were measured with the H-ADCP. Some significant peaks can also be identified. It is mostly likely that ARPAE sampling missed those SSC peaks, thus resulting in an underestimation of the sediment load, especially in November, due to the short duration of the peak events. This puts in evidence the need of continuous river monitoring.

3.5 Analysis of hydrological events

The possibility of continuous monitoring of flow rate and SSC allows measuring hydrological events. Furthermore, by measuring simultaneously different variables it becomes possible to analyse how they interact. Two of these variables are the flow rate, Q and SSC. Figure 8 (a) and (b) shows flow rate and SSC time-series for both rivers (Sec-

chia and Devoll), for a two month period between November and December 2017. In Figure 8 different events are identified, S1 to S7 for Secchia and D1 to D7 for Devoll. It is possible to see that both variables are correlated. However, the peak of flow rate does not coincide necessarily with the peak of SSC. A more detailed analysis can be made by plotting Q vs SSC as suggested by Williams (1989) and used by several other authors (e.g. Lloyd et al. (2016); Juez et al. (2018); Matos et al. (2018)) to analyse the sediment transport processes.

Williams (1989) proposed that the curves Q-SSC fall into one of 5 classes, depending on the behaviour of Q and SSC. These classes are: (i) single value, indicating no difference in the sediment transport rate between the rising and falling limbs of the hydrograph; (ii) clockwise hysteresis, when the sediment transport in the rising limb of the hydrograph is greater; (iii) counterclockwise hysteresis, meaning a greater sediment transport rate on the falling limb of the hydrograph; (iv) a single value plus a loop, resulting of combining (i) and either (ii) or (iii); and (v) a 8-shaped figure which is a result of combining (ii) and (iii).

Seven events were identified on the Secchia, S1 to S7, in the period November-December 2017. As it can be seen, November was a quite dry month, as the water level was often below the H-ADCP location. The first three events, from which only S1 is depicted in Figure 10 (a), showed an "8-shaped" figure hysteresis and the others (S4-S7) a clockwise hysteresis curve (S2).

The hysteresis curves obtained for the Devoll have shown a more complex case as illustrated in Figure 10 (b). Whereas in the Secchia case, configurations (ii) and (iii) were well defined, in the Devoll, for the identified events, a mix of configurations of hysteresis curves was found. For example, for case D1 (Figure 10 (b)) the sedigraph starts as clockwise, but after the loop it starts to look counterclockwise. Event D2 starts clockwise, but an "8-shaped" figure is also observable before the sedigraph resumes its original clockwise tendency. This is related with the other peaks observed in the sedigraph time series (Figure 8). Event D6 shows a quite complicated situation, as it can be seen in Figure 10 (b), which translates the variation of the corresponding hydrograph and sedigraph. Due to the method's limitations, the sharp rise of the concentration of event D3 could not be captured. The hydrograph peaks corresponding to events D4, D5 and D6 is much smaller than D3. It seems that is this latter event that triggers the high SSC

measured from December 3rd to December 23rd and events D4 to D6 only contribute to keep those high values of SSC.

4 Discussion

4.1 ABR-method: advantages and limitations

The ABR-method using H-ADCP is an improvement of the attenuation method, due to the introduction of the conversion function between ABR and ζ_s. This conversion function empirically accounts for organic and inorganic percentage suspended into measurement volume besides PSD variations. This method is useful in case of limited channel width and negligible SSC gradients where the H-ADCP can be used to concurrently estimate flow discharge and SSC that enable sediment flux estimation.

Measurements of H-ADCPs within monitoring stations at two very different case studies bore out that the ABR-method may provide the continuous evaluation of suspended sediment fluxes. The flow rate is calculated from the measured velocity profiles, while the SSC is computed from the resulting echo profiles, being both measurements carried at the same time instants. In fact, the success of using an ADCP for SSC estimation is because of echo profiling is a by-product of flow discharge measurement, therefore SSC and flow discharge may be assessed from the same measuring that are based on suspended particles backscatter and the Doppler shift of received signal, respectively. However, this advantage is balanced from the lack of a detailed knowledge of instrumental parameters which are needed for the inversion of the sonar equation and the large volume of ensonified water. This makes challenging and possibly inaccurate the inversion of the sonar equation. Therefore, using an ADCP for SSC measurements appears relevant when the contemporaneous assessment of flow discharge is possible. Otherwise, the using of dedicated probes for small scale (i.e., punctual and short profile volume of measurement) and continuous estimation of SSC appear more convenient (e.g., multi-frequency acoustic probe AQUAscat produced by Aquatec Group Ltd, UK).

Very short echo profiles may also prevent the evaluation of sound attenuation and, consequently, the application of the proposed ABR-method for SSC assessment. This was exactly the case of very high peak observed at the Devoll River between the end of November and the beginning of December 2017 (Figure 8 (b)) when the H-ADCP profiling was impossible due to the noise level (i.e., a flat echo return). In this condition no

profile measurement was available, however, the peak discharge was extrapolated from the rating curve water level vs Q, (i.e., $\approx 10^3\,\mathrm{m^3 s^{-1}}$ Figure 8 (b)), while the SSC evaluation lacked. In fact, no trivial relation exist between flow discharge and SSC (Figure 9) which hindered the extrapolation of a rough estimation for SSC. The observed degradation of echo profiles appears related to the noise level that was particularly relevant at the Devoll River during floods. The maximum velocity measured at the Kokel monitoring station was about 4 $\mathrm{ms^{-1}}$, the peak flow exceeding that value likely mobilized cobbles and produced relevant turbulence close to the channel bed. In these conditions, the emitted pulses from H-ADCP were likely decorrelated resulting in scarce return and low signal to noise ratio (Brumley et al., 1991; Conevski et al., 2019). The displacement of the H-ADCP to a higher level, away from the bed turbulence, may be a practical solution to increase the signal to noise ratio which would enable the profile measurement even for highest peaks. Alternately, a small scale acoustic probe may be integrated to eventually provide a punctual measurement of SSC for those cases. It's worth noting that small scale acoustic probes ensonify a reduced water volume that limits sound spreading and attenuation, eventually facilitating the detection of backscattering strength from suspended matter.

Regarding sound attenuation, at the Devoll River two H-ADCPs were used working at 0.6 MHz and 1.2 MHz. No relevant gain was observed in terms of sound penetration into water column for the lower frequency, indeed few additional estimations of SSC were available for the 0.6 MHz, but the very high peak was lost in both cases. On the other hand, the higher tone produced a more detailed water velocity profile close to the left bank, which was used to estimate the flow discharge with the index method. This is because the 1.2 MHz has a spatial resolution of 0.5 m and the blanking distance (i.e., the not measured portion close to instrument head) is limited to about 0.5 m - 0.8 m while these parameters double for the 0.6 MHz H-ADCP.

Summarizing: in case of very high discharge values the method failed in measuring both the parameters that was because of too low signal to noise ratio, whereas it successfully estimated SSC within three orders of magnitude from $10^{-1}\,\mathrm{gl^{-1}}$ to $10^{1}\,\mathrm{gl^{-1}}$ and the corresponding cumulated sediment fluxes across the river channel. The H-ADCP working at 1.2 MHz would be the best choice in case of the Kokel monitoring station: the flow discharge assessment was much more reliable and no relevant differences were observed

for SSC evaluations from the two frequencies, although the ABR-method application was more robust with 0.6 MHz echo profiles.

In the Secchia, the signal to noise ratio measured was always above 10 dB. This allowed the H-ADCP to track the flood peaks. Discontinuities in the time-series were due to water levels below the H-ADCP level.

4.2 Discussion of single hydrological events

Juez et al. (2018) showed that one of the main drivers of the hysteretical behavior in the Q-SSC plots is the ratio between the sediment distal supply and the proximal sediment availability. According to Williams (1989) and Reid et al. (2016), clockwise hysteresis is due to depletion or flush of fine sediments in the channel, and counterclockwise is related with channel aggradation.

The Secchia River results (Figure 10 (a)) are easier to analyse since the phase plots are easier to interpret. Event S1 exemplifies a 8-figure event. It starts in a counterclockwise manner, indicating that there is aggradation, but then it becomes for a while clockwise orientated, and resuming its counterclockwise nature. The counterclockwise orientation could be linked to the distal supply that would deposit at the monitoring station location, followed by a small flush of local sediment to explain the short clockwise orientation, to then be resumed in a counterclokwise manner. Depicted events S4 and S7 are both clockwise, indicating depletion of fine sediments of the channel.

For the Devoll, the identified events appear more complex. There are probably some localized events that seem to be imposed on a specific feature, for example, in event D2 (Figure 10 (b)), the event is globally clockwise orientated, however there is a part where the phase-plot becomes quite irregular. The same happening with event D6.

The Devoll is a mountain river, with steep slopes. Downstream of the measuring station, some landslides were reported during the month of December. Due to the instability of the river banks, it is reasonable to assume, that some of the erratic behaviour of the phase plots Q-SSC can be related to slope instabilities and consequent sediment input. This however needs to be studied in further detail and with extra monitoring capabilities.

5 Conclusions

An acoustic method to measure the SSC based on the attenuation to backscatter ratio (ABR) of sound emitted by a H-ADCP was applied to two different rivers: Secchia, a lowland river in Italy and the Devoll, a mountain river in Albania.

The typical acoustic sensitivity to PSD, which burdens the ADCP based methods applicability, was limited. Further analysis was made on the nature of the suspended matter. This analysis allowed to investigate the fraction of inorganic to organic materials presented in the water volume. Despite the limited number of samples available for detailed laboratory analyses, it was possible to investigate the effect of the organic material in the ADCP profiling. For the first time, the organic/inorganic content was accounted for to improve the ABR-method for SSC estimation. Further research is needed to assess the possibility of extending the proposed SSC acoustic method to measure both inorganic and organic concentrations.

The results coming from two measuring stations of two different rivers of the Adriatic basin were analysed. This analysis consisted in determining the water level, and flow rate using the index-method. The ABR-method was applied to extract the SSC as a by-product of the echo profiles measured with the ADCP. To the authors' best knowledge, this is the first time that such systematic analysis is made for two different rivers. Due to its continuous measurement nature, a sediment budget for the Secchia and the Devoll was calculated. Results shown that, by using the ARPAE data for the Secchia River, based on infrequent sampling, the obtained sediment budget is underestimated. This stresses the need for continuous nmeasurements.

With the obtained time-series it was shown to be possible to measure single hydrological events. The phase plots Q-SSC were drawn for both rivers, yielding some hysteresis curves. These curves have shown that the Secchia, a lowland river, appears to have a more regular behaviour than the Devoll. Furthermore, for the case of the Devoll, some phase plots were shown to be quite irregular. This can be due to localized events (e.g. landslides) that locally change the sediment input. However, further investigation on these hydro-morphological processes is still required.

Acronyms

ABR attenuation-to-backscatter ratio

ARPAE Agenzia Regionale per la Prevenzione, l'Ambiente e l'Energia dell'Emilia-Romagna, Regional Agency for Prevention, Environment and Energy of Emilia-Romagna.

H-ADCP horizontal/side looking acoustic Doppler current profiler

PSD particle-size distribution

SSC suspended sediment concentration

USGS United States Geological Survey

Notation

$\boldsymbol{\alpha_s}$ sediment attenuation coefficient

$\boldsymbol{\alpha_w}$ water attenuation coefficient

$\boldsymbol{\zeta_s}$ normalized attenuation coefficient

$\boldsymbol{\sigma_s^2}$ backscatter

$\boldsymbol{\psi}$ correction factor for near-field, for far-field $\psi = 1$.

$\boldsymbol{d}$ diameter

$\boldsymbol{I_{\mathrm{dB}}}$ echo intensity level profile

$\boldsymbol{K}$ instrumental constant

$\boldsymbol{k_s^2}$ backscatter strength coefficient

$\boldsymbol{C}$ suspended sediment concentration

$\boldsymbol{Q}$ flow rate

$\boldsymbol{r}$ ranging distance

$\boldsymbol{skw}$ skewness of the sediments' diameters distribution

$\boldsymbol{std}$ sediments' diameter standard deviation

Acknowledgments

This research has been developed in the framework of the projects: (i) Sedipass 2015-2018 funded by the Norwegian Research Council and Statkraft and (ii) INFRASAFE - Monitoraggio intelligente per infrastrutture sicure, April 2016 - March 2018, funded by the Emilia-Romagna Region of Italy, through the POR FESR 20142020.

Part of the work performed by Michael Nones was developed within the statutory activities No. 3841/E-41/S/2018 of the Ministry of Science and Higher Education of Poland.

The authors would like to thank the three anonymous reviewers and the Associate Editor for the valuable comments and feedback.

The data used in this paper can be downloaded from the following server:

https://1drv.ms/f/s!AlxV78bmdJpZhBfEs4FZ1FrB-Uiu.

References

Agrawal, Y. C., & Hanes, D. M. (2015). The implications of laser-diffraction measurements of sediment size distributions in a river to the potential use of acoustic backscatter for sediment measurements. *Water Resources Research*, *51*(11), 8854-8867. Retrieved from `https://agupubs.onlinelibrary.wiley.com/doi/abs/10.1002/2015WR017268` doi: 10.1002/2015WR017268

Aleixo, R., Guerrero, M., & Ruther, N. (2019). The long-term monitoring of suspended sediment transport with side looking ADCP - a GUI for echo profiles interpretation. In A. Radice (Ed.), *Proceedings of the HydroSenSoft Conference.* Madrid, Spain.

Almestad, C. (2015). *Modelling of water allocation and availability in Devoll river basin, Albania* (Master thesis). NTNU Norwegian University of Science and Technology, Norway.

ARPAE. (2017). *Annali idrologici parte seconda* (Tech. Rep.). Agenzia Regionale per la prevenzione, l' ambiente e l' energia dell' Emilia Romagna.

Brumley, B., Cabrera, R., Deines, K., & Terray, E. (1991). Performance of a broadband acoustic doppler current profiler. *IEEE Journal of Oceanic Engineering*, *16*, 402-407. doi: 10.1109/48.90905

Bux, J., Peakall, J., Rice, H., Manga, M., Biggs, S., & Hunter, T. (2019). Measurement and density normalisation of acoustic attenuation and backscattering constants of arbitrary suspensions within the rayleigh scattering regime. *Applied Acoustics*, *146*, 9-22.

Comiti, F., Mao, L., Penna, D., Dell'Agnese, A., Engel, M., Rathburn, S., & Cavalli, M. (2019). Glacier melt runoff controls bedload transport in alpine catchments. *Earth and Planetary Science Letters*, *520*, 77 - 86. Retrieved from `http://www.sciencedirect.com/science/article/pii/S0012821X19303012` doi: https://doi.org/10.1016/j.epsl.2019.05.031

Conevski, S., Guerrero, M., Ruther, N., & Rennie, C. (2019). Laboratory investigation of the apparent bedload velocity measured by adcps. *Journal of Hydraulic Engineering*. doi: 10.1061/(ASCE)HY.1943-7900.0001632

Elhakeem, M., Papanicolaou, A. T., & Wilson, C. G. (2017). Implementing streambank erosion control measures in meandering streams: design procedure enhanced with numerical modelling. *International Journal of River Basin Management*, *15*(3), 317-327. Retrieved from `https://doi.org/10.1080/15715124.2017.1315816` doi: 10.1080/15715124.2017.1315816

Felix, D., Albayrak, I., & Boes, R. M. (2016). Combining in-situ laser diffraction (lisst) and vibrating tube densimetry to measure low and high suspended sediment concentrations. In *Proceedings of International Symposium on River Sedimentation, Stuttgart, Germany.*

Flammer, G. H. (1962). Ultrasonic measurement of suspended sediment. *U.S. Geol. Surv. Bull*, *1141-A*.

Fritsch. (2016). Operating instructions analysette 22 laser particle sizer Fritsch nanotec [Computer software manual].

Guerrero, M., & DiFederico, V. (2018). Suspended sediment assessment by combining sound attenuation and backscatter measurements analytical method and experimental validation. *Advances in Water Resources*, *113*, 167-179. doi: 10.1016/j.advwatres.2018.01.020

Guerrero, M., Latosinski, F., Nones, M., Szupiany, R. N., Re, M., & Gaeta, M. G. (2015). A sediment fluxes investigation for the 2-d modelling of large river morphodynamics. *Advances in Water Resources*, *81*, 186 - 198. Retrieved from `http://www.sciencedirect.com/science/article/pii/S0309170815000196` (Fluvial Eco-Hydraulics And Morphodynamics) doi: https://doi.org/10.1016/j.advwatres.2015.01.017

Guerrero, M., Rüther, N., Haun, S., & Baranya, S. (2017). A combined use of acoustic and optical devices to investigate suspended sediment in rivers. *Advances in Water Resources*, *102*, 1 - 12. Retrieved from `http://www.sciencedirect.com/science/article/pii/S0309170816302731` doi: https://doi.org/10.1016/j.advwatres.2017.01.008

Guerrero, M., Ruther, N., Szupiany, R., Haun, S., Baranya, S., & Latosinski, F. (2016). The acoustic properties of suspended sediment in large rivers:

Consequences on adcp methods applicability. *Water-MDPI*, *8*, 13. doi: 10.3390/w8010013

Guerrero, M., Szupiany, R., & Latosinski, F. (2013). Multi-frequency acoustics for suspended sediment studies: an application in the Parana River. *Journal of Hydraulic Research*, *51*(6), 696-707. Retrieved from https://doi.org/10.1080/00221686.2013.849296 doi: 10.1080/00221686.2013.849296

Haimann, M., Hauer, C., Tritthart, M., Prenner, D., Leitner, P., Moog, O., & Habersack, H. (2016). Monitoring and modelling concept for ecological optimized harbour dredging and fine sediment disposal in large rivers. *Hydrobiologia*. doi: 10.1007/s10750-016-2935-z

Head, K. (2006). *Manual of soil laboratory testing volume 1 soil classification and compaction tests* (3rd ed., Vol. 1). CRC Press Boca Raton, Florida, USA.

Horowitz, A. J. (2003). An evaluation of sediment rating curves for estimating suspended sediment concentrations for subsequent flux calculations. *Hydrological Processes*, *17*(17), 3387-3409. Retrieved from https://onlinelibrary.wiley.com/doi/abs/10.1002/hyp.1299 doi: 10.1002/hyp.1299

IRSA-CNR. (2003). *Metodi analitici per le acque, sezione 2000 parametri chimico-fisici, 2090 solidi* (Tech. Rep.). Author. Retrieved from www.gtdambiente.it/content/docs/norme_e_metodi/APAT-CNR-IRSA/file/2090.pdf

Juez, C., Hassan, M., & Franca, M. (2018). The origin of fine sediment determines the observations of suspended sediment fluxes under unsteady flow conditions. *Water Resources Research*(54), 5654-5669. doi: 10.1029/2018wr022982

Kinsler, L., Frey, A. R., Coppens, A. B., & Sanders, J. V. (2000). *Fundamentals of acoustics*. John Wiley and Sons.

Levesque, V., & Oberg, K. (2012). *Computing discharge using the index velocity method. techniques and methods report 3a2348* (Tech. Rep.). USGS. Retrieved from http://pubs.usgs.gov/tm/3a23/

Lloyd, C., Freer, J., Johnes, P., & Collins, A. (2016). Using hysteresis analysis of high-resolution water quality monitoring data, including uncertainty, to infer controls on nutrient and sediment transfer in catchments. *Science of the Total Environment*. doi: 10.1016/j.scitotenv.2015.11.028

Matos, J. P., Hassan, M. A., Lu, X. X., & Franca, M. J. (2018). Probabilistic prediction and forecast of daily suspended sediment concentration on the upper

Yangtze River. *Journal of Geophysical Research: Earth Surface*, *123*(8), 1982-2003. Retrieved from https://agupubs.onlinelibrary.wiley.com/doi/abs/10.1029/2017JF004240 doi: 10.1029/2017JF004240

Medwin, H., & Clay, C. S. (1998). *Fundamentals of acoustic oceanography*. Academic Press.

Milliman, J. D., Bonaldo, D., & Carniel, S. (2016). Flux and fate of river-discharged sediments to the adriatic sea. *Advances in Oceanography and Limnology*, *7(2)*, 106-114. doi: 10.4081/aiol.2016.5899

Moore, S., Coz, J. L., Hurther, D., & Paquier, A. (2012). On the application of horizontal adcps to suspended sediment transport surveys in rivers. *Continental Shelf Research*, *46*, 50 - 63. Retrieved from http://www.sciencedirect.com/science/article/pii/S0278434311003335 (The application of acoustics to sediment transport processes) doi: https://doi.org/10.1016/j.csr.2011.10.013

Nones, M., & Gerstgraser, C. (2016). Morphological changes of a restored reach: The case of the Spree River, Cottbus, Germany. *GeoPlanet: Earth and Planetary Sciences*, 167-182.

NORCONSULT, D. H. . (2011). *ESIA Final Report - Executive summary. Devoll Hydropower Project, Engineering services - development phase* (Tech. Rep.). Norway: NORCONSULT.

Paarlberg, A. J., Guerrero, M., Huthoff, F., & Re, M. (2015). Optimizing dredge-and-dump activities for river navigability using a hydro-morphodynamic model. *Water*(7), 3943:3962. doi: 10.3390/w7073943

Rainato, R., Picco, L., Cavalli, M., Mao, L., Neverman, A. J., & Tarolli, P. (2018). Coupling climate conditions, sediment sources and sediment transport in an alpine basin. *Land Degradation & Development*, *29*(4), 1154-1166. Retrieved from https://onlinelibrary.wiley.com/doi/abs/10.1002/ldr.2813 doi: 10.1002/ldr.2813

Reid, D. A., Hassan, M. A., & Floyd, W. (2016). Reach-scale contributions of road-surface sediment to the Honna River, Haida Gwaii, bc. *Hydrological Processes*, *30*(19), 3450-3465. Retrieved from https://onlinelibrary.wiley.com/doi/abs/10.1002/hyp.10874 doi: 10.1002/hyp.10874

Sassi, M. G., Hoitink, A. J. F., & Vermeulen, B. (2012). Impact of sound attenuation by suspended sediment on ADCP backscatter calibrations. *Water*

Resources Research, *48*(9). Retrieved from https://agupubs.onlinelibrary.wiley.com/doi/abs/10.1029/2012WR012008 doi: 10.1029/2012WR012008

Sequoia. (2018). LISST-portable XR manual, version 1.3, [Computer software manual].

Sigurd, S. (2017). *New techniques for estimating sediment load for the catchment of Banja HPP* (Master thesis). NTNU Norwegian University of Science and Technology, Norway.

Szupiany, R. N., Lopez Weibel, C., Guerrero, M., Latosinski, F., Wood, M., Dominguez Ruben, L., & Oberg, K. (2019). Estimating sand concentrations using ADCP-based acoustic inversion in a large fluvial system characterized by bi-modal suspended-sediment distributions. *Earth Surface Processes and Landforms*, *44*(6), 1295-1308. Retrieved from https://onlinelibrary.wiley.com/doi/abs/10.1002/esp.4572 doi: 10.1002/esp.4572

Thorne, P. D., & Hanes, D. M. (2002). A review of acoustic measurement of small-scale sediment processes. *Continental Shelf Research*, *22*(4), 603 - 632. Retrieved from http://www.sciencedirect.com/science/article/pii/S0278434301001017 doi: https://doi.org/10.1016/S0278-4343(01)00101-7

Thorne, P. D., & Meral, R. (2008). Formulations for the scattering properties of suspended sandy sediments for use in the application of acoustics to sediment transport processes. *Continental Shelf Research*, *28*(2), 309 - 317. Retrieved from http://www.sciencedirect.com/science/article/pii/S0278434307002634 doi: https://doi.org/10.1016/j.csr.2007.08.002

Urick, R. J. (1948). The absorption of sound in suspensions of irregular particles. *J. Acoust. Soc. Am*, *20*(3), 283-289.

Venditti, J. G., Church, M., Attard, M. E., & Haught, D. (2016). Use of adcps for suspended sediment transport monitoring: An empirical approach. *Water Resources Research*, *52*(4), 2715-2736. Retrieved from https://agupubs.onlinelibrary.wiley.com/doi/abs/10.1002/2015WR017348 doi: 10.1002/2015WR017348

Williams, G. P. (1989). Sediment concentration versus water discharge during single hydrologic events in rivers. *Journal of Hydrology*, *111*(1), 89 - 106. Retrieved from http://www.sciencedirect.com/science/article/pii/

0022169489902540 doi: https://doi.org/10.1016/0022-1694(89)90254-0

Wright, S., Topping, D. T., & Williams, C. A. (2010). Discriminating silt-and-clay from suspended-sand in rivers using side-looking acoustic profilers. In *Proceedings of the 2nd joint federal interagency sedimentation conference.* Retrieved from http://acwi.gov/sos/pubs/2ndJFIC.

Table 1. Comparison of sediment budgets passing across the Secchia River at Ponte Motta as assessed from continuous H-ADCP monitoring and infrequent sampling from ARPAE. ARPAE* refers to values calculated from ARPAE data.

		SSC (g/l)		Cumulated load (ton)	
		ARPAE	H-ADCP	ARPAE*	H-ADCP
Nov 2017	max	2.00	7.06	4.2	42.4
	min	0.03	0.17		
	mean	0.13	2.7		
Dec 2017	max	2.30	5.57	158.8	234.9
	min	0.03	0.02		
	mean	1.01	1.13		

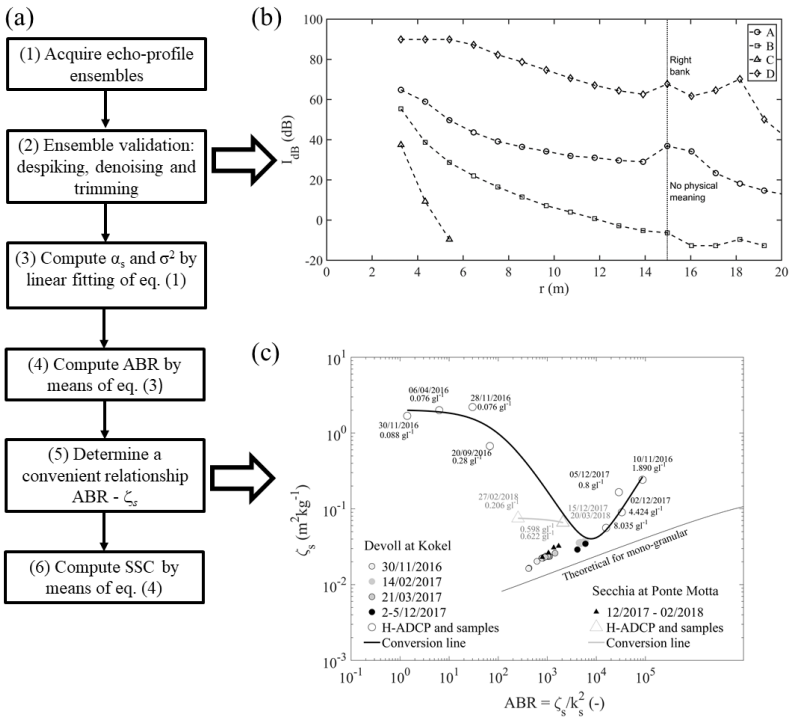

Figure 1. (a) Flowchart of operations to convert echo profiles into SSC. (b) Example of different echo profiles and the trimming operation to limit profiles to the flow region. (c) Theoretical and empirical relationships ABR-ζ_s.

Figure 2. (a) Map of the Adriatic sea with the indication of Italy and Albania, together with the estuaries of Po and Seman rivers. (b) Close up of the Secchia and Po rivers with the indication of the Ponte Motta measurement station (red dot). (c) Close up of the Devoll and Seman rivers with the indication of the measurement station at Kokel (red dot).

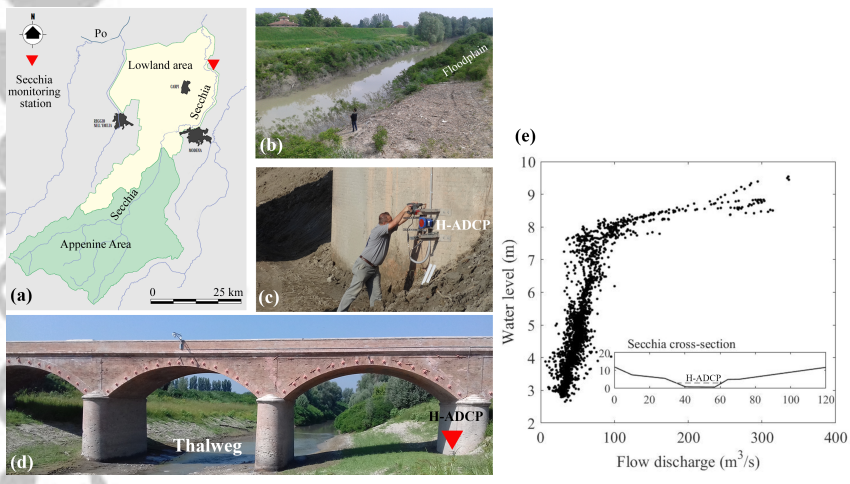

Figure 3. (a) Map of the Secchia River drainage basin from ARPAE, 2017. (b) Overview of the Ponte Motta upstream section of the river. (c) Installation of the H-ADCP. (d) Ponte Motta (bridge) and the location of the H-ADCP. (e) Rating curve and cross-section also indicating the H-ADCP level at 2.8 m referred to the local system, the dashed line represents the acoustic beams crossing path.

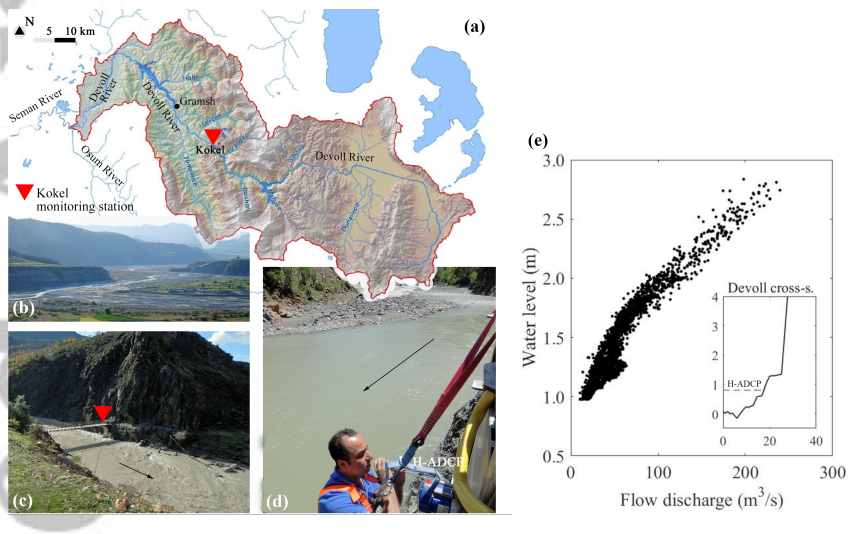

Figure 4. (a) The Devoll River map from NORCONSULT (2011) with indication of the Kokel monitoring. (b) The Devoll River downstream the monitoring station. (c) Location of the monitoring station. (d) Installation of the H-ADCP at Kokel monitoring station. (e) Rating curve and cross-section also indicating the H-ADCP level at 0.8 m referred to the local system, the dashed line represents the acoustic beams crossing path.

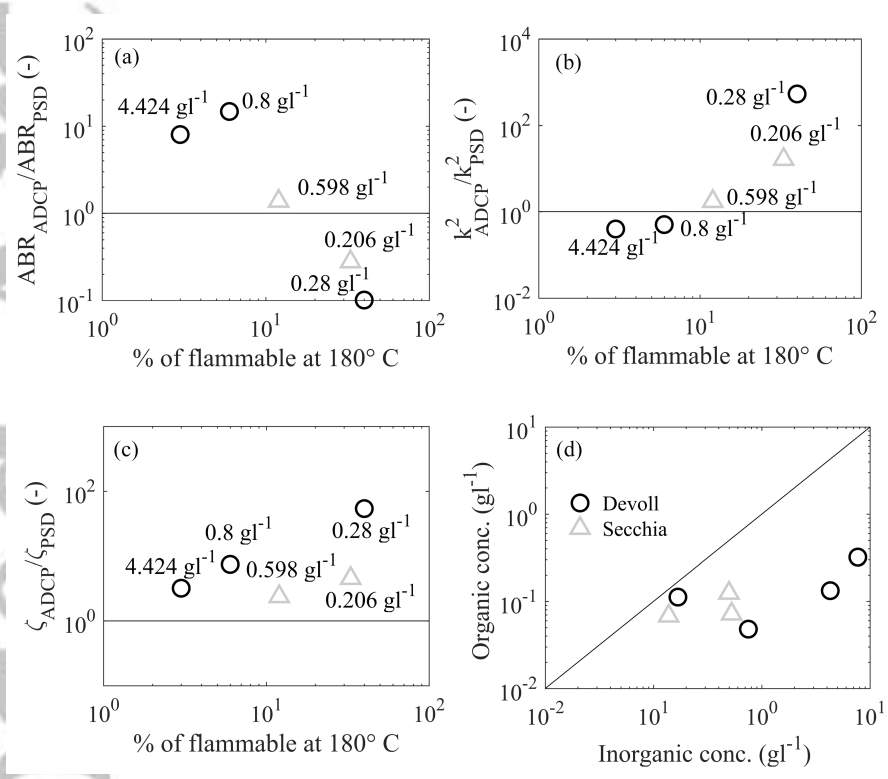

Figure 5. Acoustic parameters as function of the organic and inorganic matter expressed as percentage of flammable material at 180°C (a) Non-dimensional ABR (b) non-dimensional backscatter coefficient (c) non-dimension normalized attenuation (d) Organic concentration vs inorganic concentration.

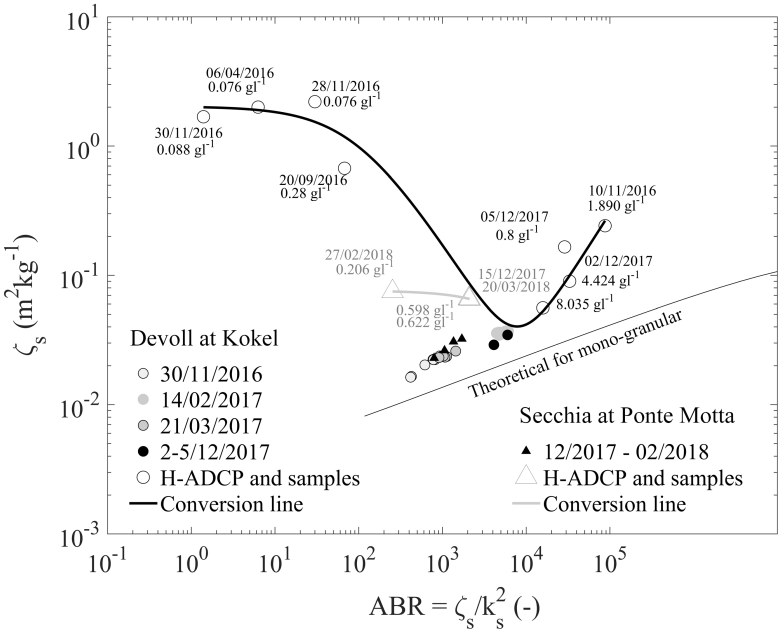

Figure 6. ABR to ζ_s conversion functions as resulted from sampled SSC and contemporaneous H-ADCP profiling for Secchia (triangles) and Devoll (open circles), and pair values from observed PSD (filled marks) at various dates.

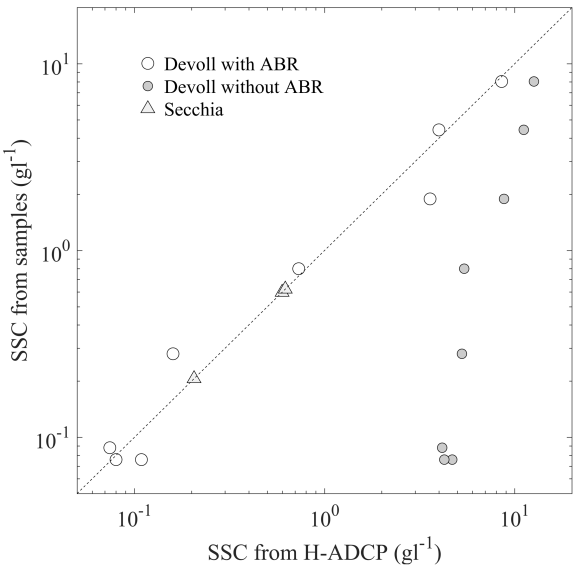

Figure 7. Comparison between acoustically inferred SSC and corresponding values from samples. The improvement of the proposed ABR-method with respect to the attenuation method which doesn't account for ABR variations is clearly visible.

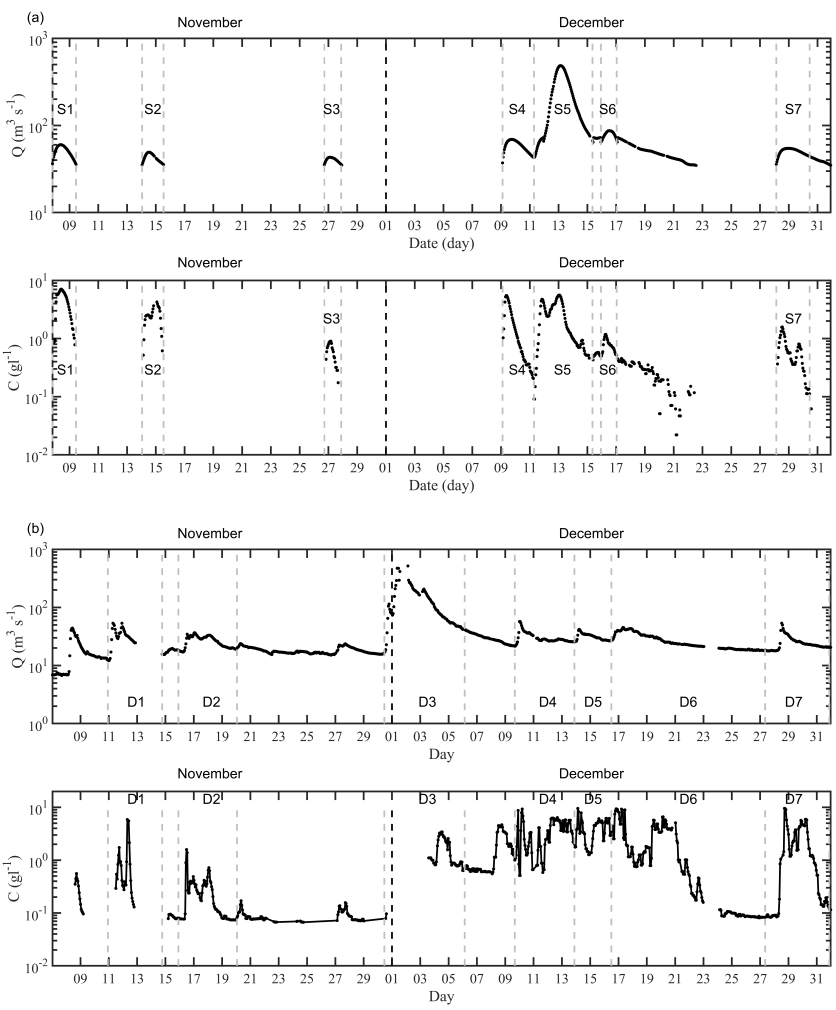

Figure 8. Time series of flow rate, Q, and SSC, C, for rivers (a) Secchia and (b) Devoll for the months November and December 2017.

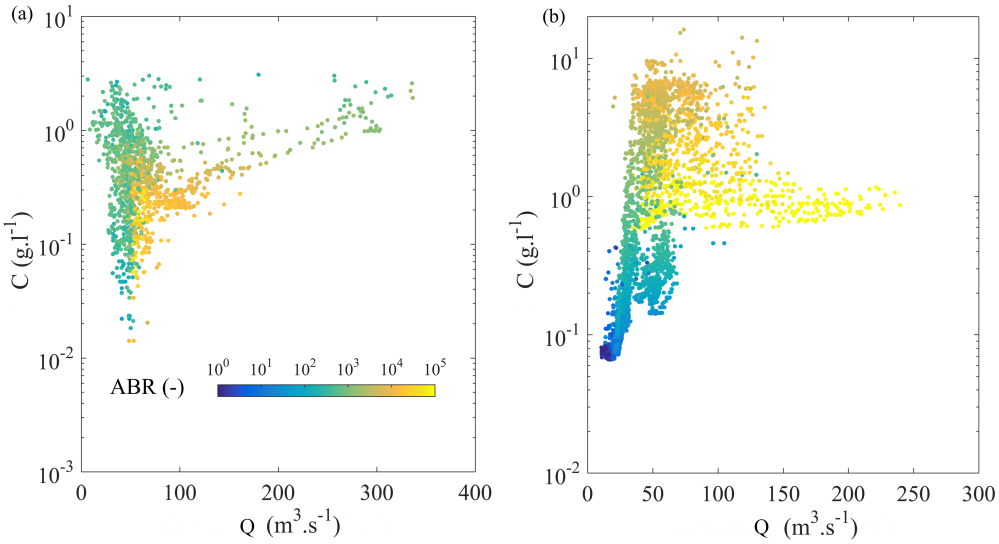

Figure 9. Flow rate (Q) versus SSC (C) distributions for (a) Secchia River and (b) Devoll River. Data is coloured as a function of the ABR.

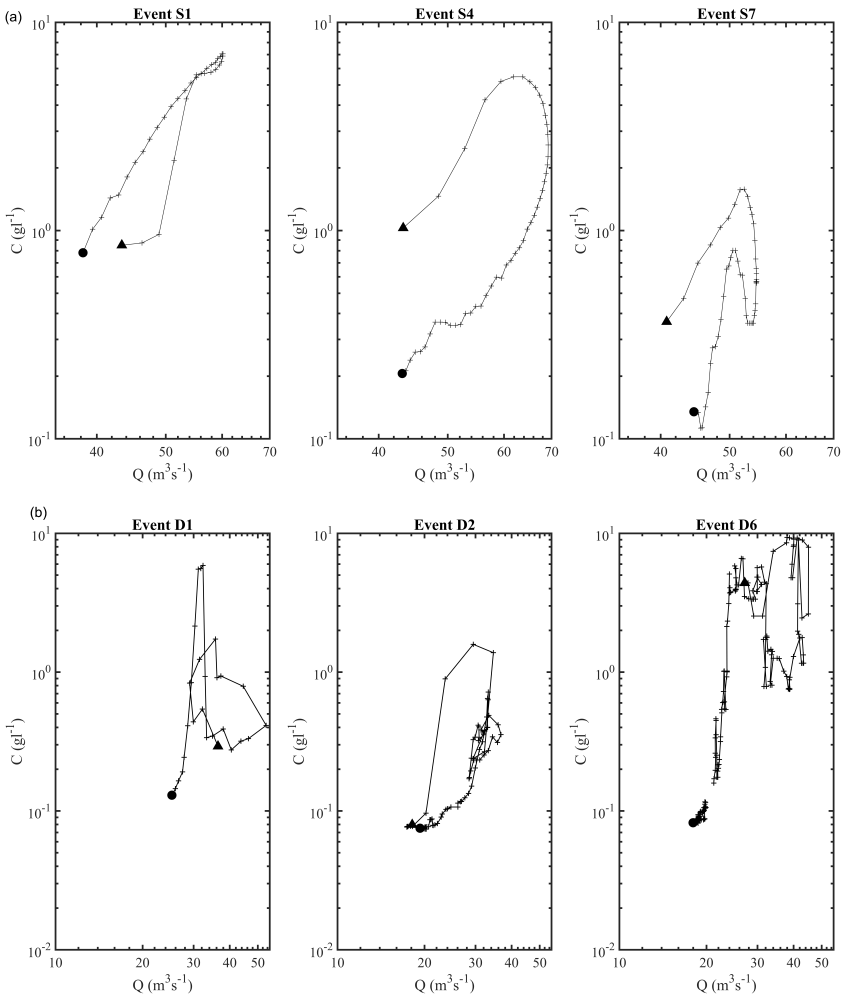

Figure 10. Analysis of three events for rivers (a) Secchia and (b) Devoll. Black triangle denotes the start of the event and the circle the end of the event.

Appendix A Secchia and Devoll surveys to assess the SSC

Table A1. List of surveys made in Devoll and in Secchia

Date	Water level (m)	Mean SSC (gl^{-1})	SSC maximal deviation*	Sampling	Technolgy for ssc assessment	Technology for PSD assessment
			Devoll			
06/04/2016	1.25	0.076	6%	-	LISST-ABS deployed in 4 positions across the river channel	-
20/09/2016	1.10	0.28	15%	-	LISST-ABS deployed close to fixed aDcp	-
10/11/2016	2.15	1.89	19%	-	LISST-ABS deployed in 3 positions across the river channel	-
28/11/2016	1.09	0.076	9%	-	LISST-ABS moving across the river channel	-
30/11/2016	1.04	0.088	63%	5 samples with P-72 sampler by USGS deployed from crossing bridge	LISST-ABS deployed in 6 positions across the river channel	Laser particle sizer Analysette 22
14/02/2017	0.99	-	-	6 samples with P-72 sampler by USGS deployed from crossing bridge	-	Laser particle sizer NTNU
21/03/2017	1.10	-	-	6 samples with P-72 sampler by USGS deployed from crossing bridge	-	Laser particle sizer Analysette 22
02/12/2017	3.70	8.035	3%	1 ISCO bottle	wet filtering and furnace drying repeated for 2 equal portions in 2 different laboratories	-
02/12/2017	3.60	4.424	34%	1 ISCO bottle	wet filtering and furnace drying repeated for 2 equal portions in 2 different laboratories	Laser particle sizer LISST portable
05/12/2017	1.80	0.8	37%	3 manual sampling with bottles deployed from crossing bridge	wet filtering and furnace drying repeated in 3 different laboratories	Laser particle sizer LISST portable
			Secchia			
17/11/2017	1.50	0.149	10%	6 sampling with Watertrap by Eijkelkamp Soil & Water deployed from crossing bridge	wet filtering and furnace drying	-
15/12/2017	7.30	0.598	5%	6 sampling with Watertrap by Eijkelkamp Soil & Water deployed from crossing bridge	wet filtering and furnace drying	Laser particle sizer Analysette 22
27/02/2018	3.10	0.206	20%	6 sampling with Watertrap by Eijkelkamp Soil & Water deployed from crossing bridge	wet filtering and furnace drying	Laser particle sizer Analysette 22
20/03/2018	8.30	0.622	5%	6 sampling with Watertrap by Eijkelkamp Soil & Water deployed from crossing bridge	wet filtering and furnace drying	-

(*) in % from mean value (different samples, positions and repeated analyses)

Figure 1 (a) Flowchart of operations to convert echo profiles into SSC. (b) Example of different echo profiles and the trimming operation to limit profiles to the flow region. (c) Theoretical and empi.

(a)

(1) Acquire echo-profile ensembles

(2) Ensemble validation: despiking, denoising and trimming

(3) Compute α_s and σ^2 by linear fitting of eq. (1)

(4) Compute ABR by means of eq. (3)

(5) Determine a convenient relationship ABR - ζ_s

(6) Compute SSC by means of eq. (4)

(b)

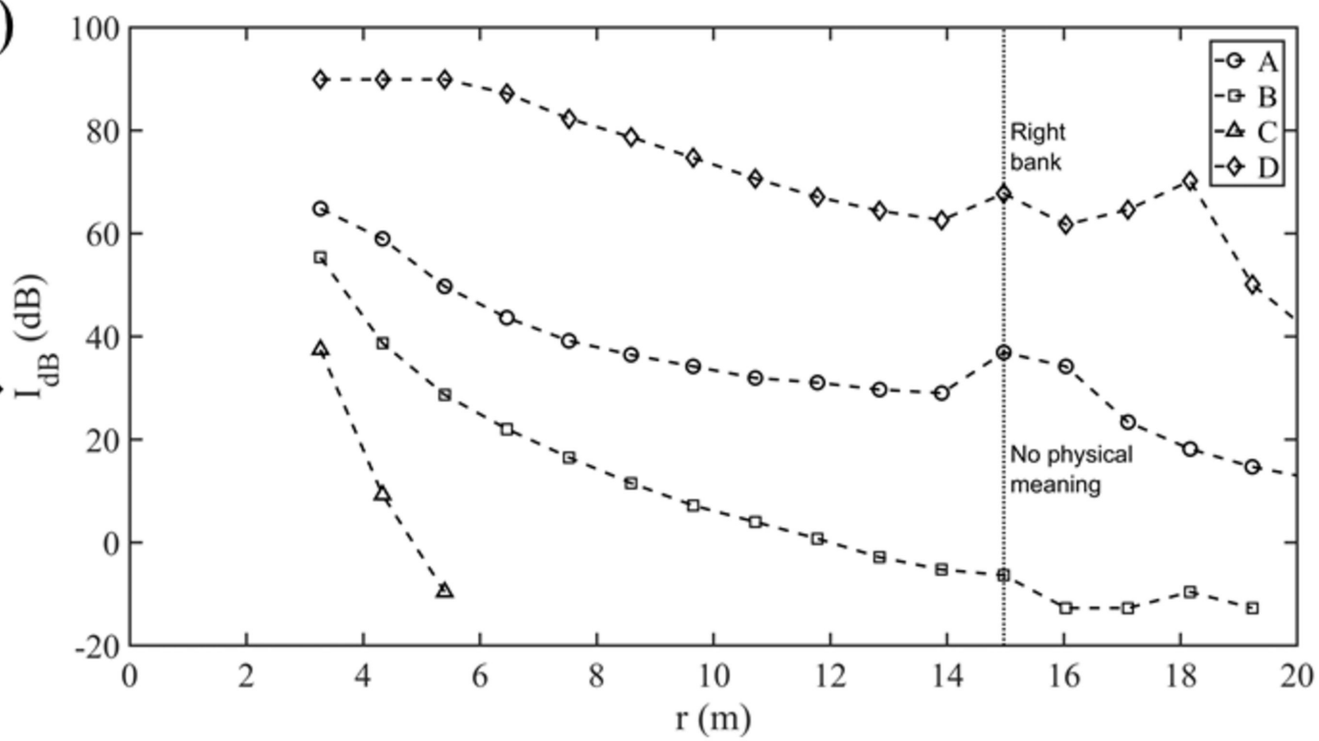

(c)

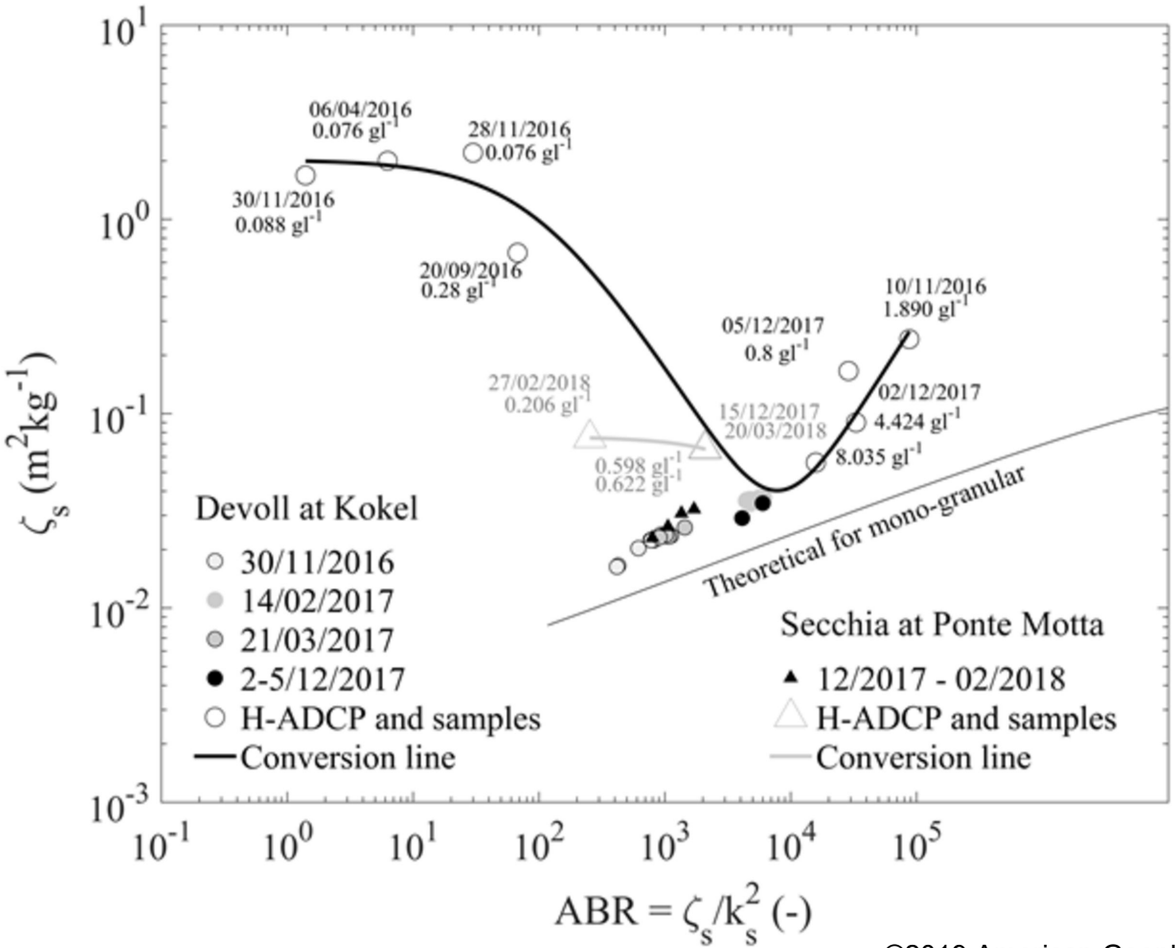

Figure 2 (a) Map of the Adriatic sea with the indication of Italy and Albania, together with the estuaries of Po and Seman rivers. (b) Close up of the Secchia and Po rivers with the indication of the.

Figure 3 (a) Map of the Secchia River drainage basin from ARPAE, 2017. (b) Overview of the Ponte Motta upstream section of the river. (c) Installation of the H-ADCP. (d) Ponte Motta (bridge) and the.

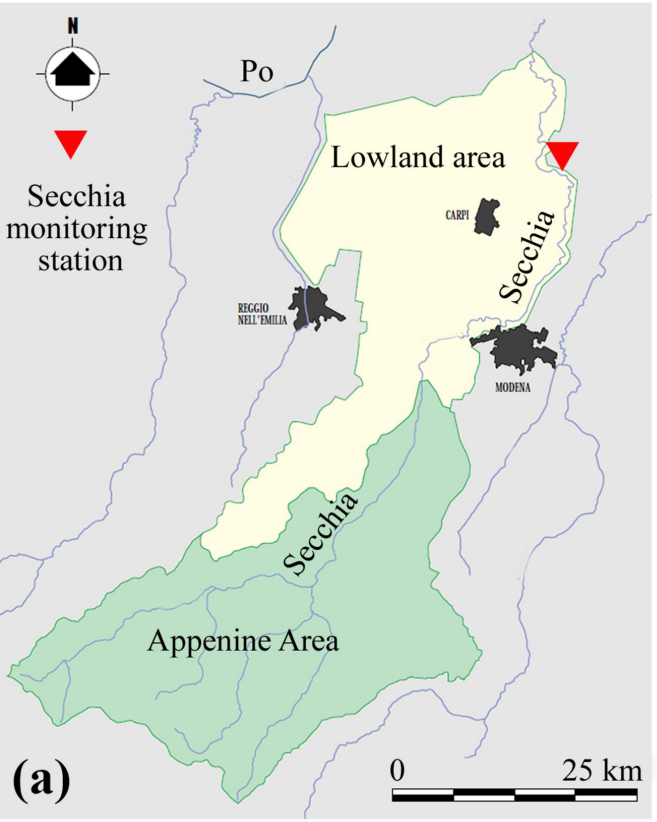

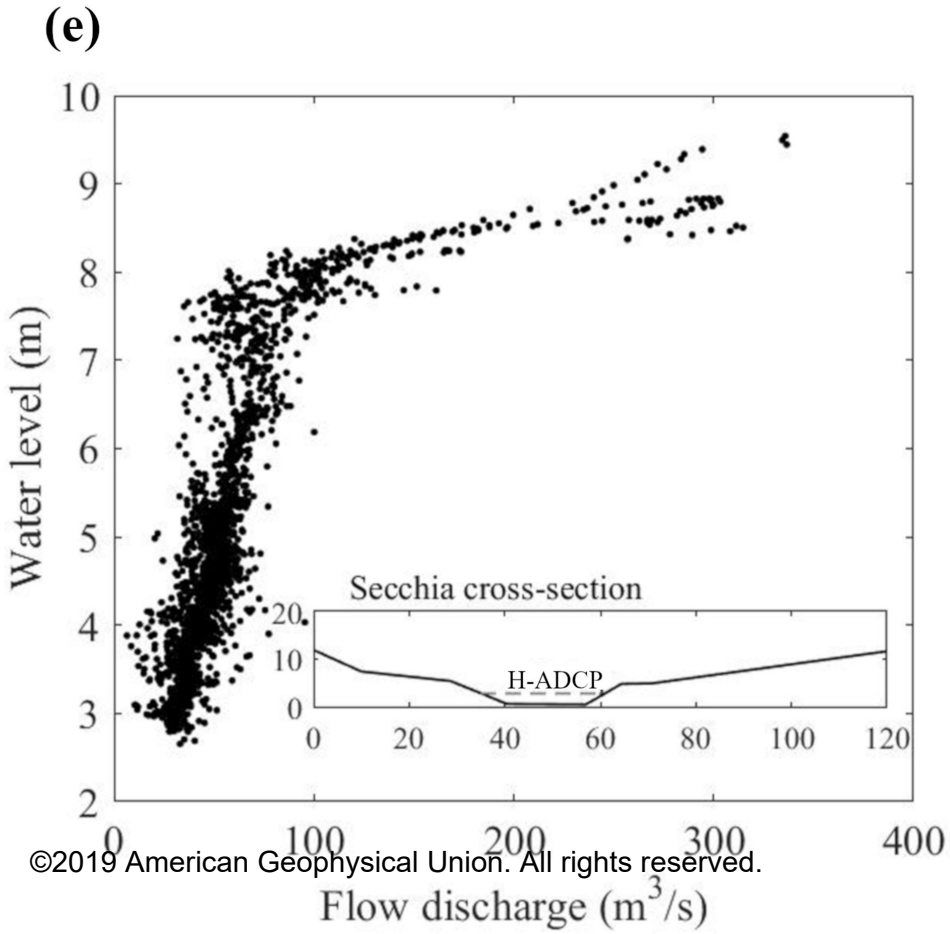

Figure 4 (a) The Devoll River map from \citeA{Devoll2011} with indication of the Kokel monitoring. (b) The Devoll River downstream the monitoring station. (c) Location of the monitoring station. (d).

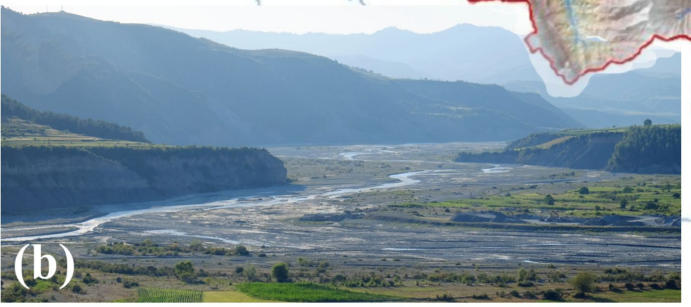

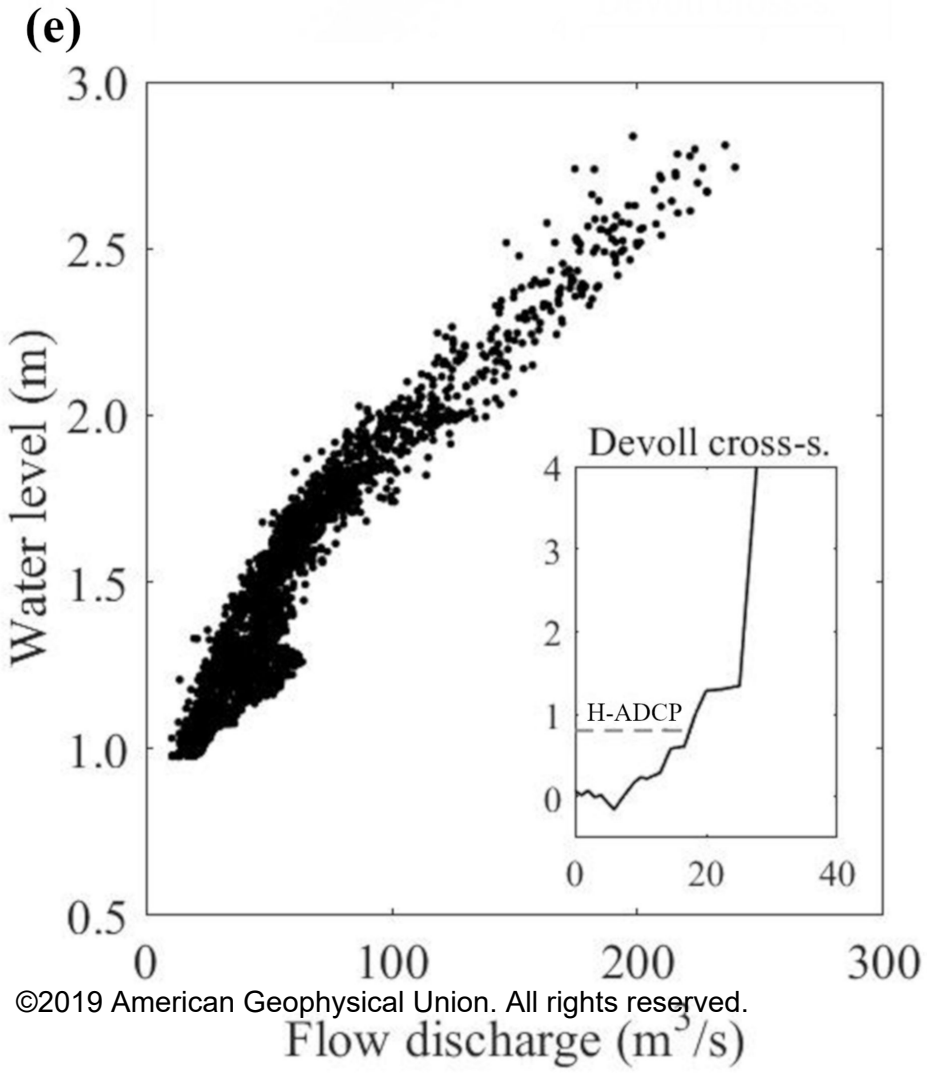

Figure 5 Acoustic parameters as function of the organic and inorganic matter expressed as percentage of flammable material at 180^{o}C (a) Non-dimensional ABR (b) non-dimensional backscatter coeffic.

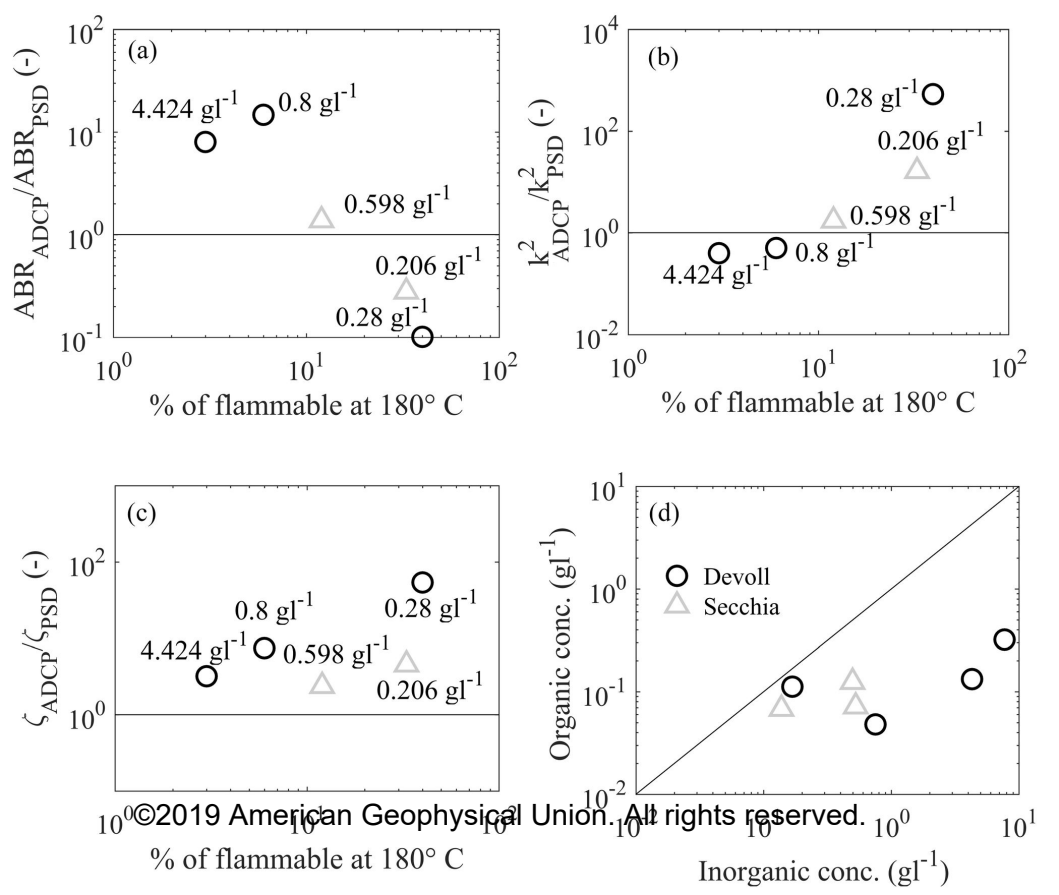

Figure 6 ABR to ζ_{s} conversion functions as resulted from sampled SSC and contemporaneous H-ADCP profiling for Secchia (triangles) and Devoll (open circles), and pair values from observed PSD.

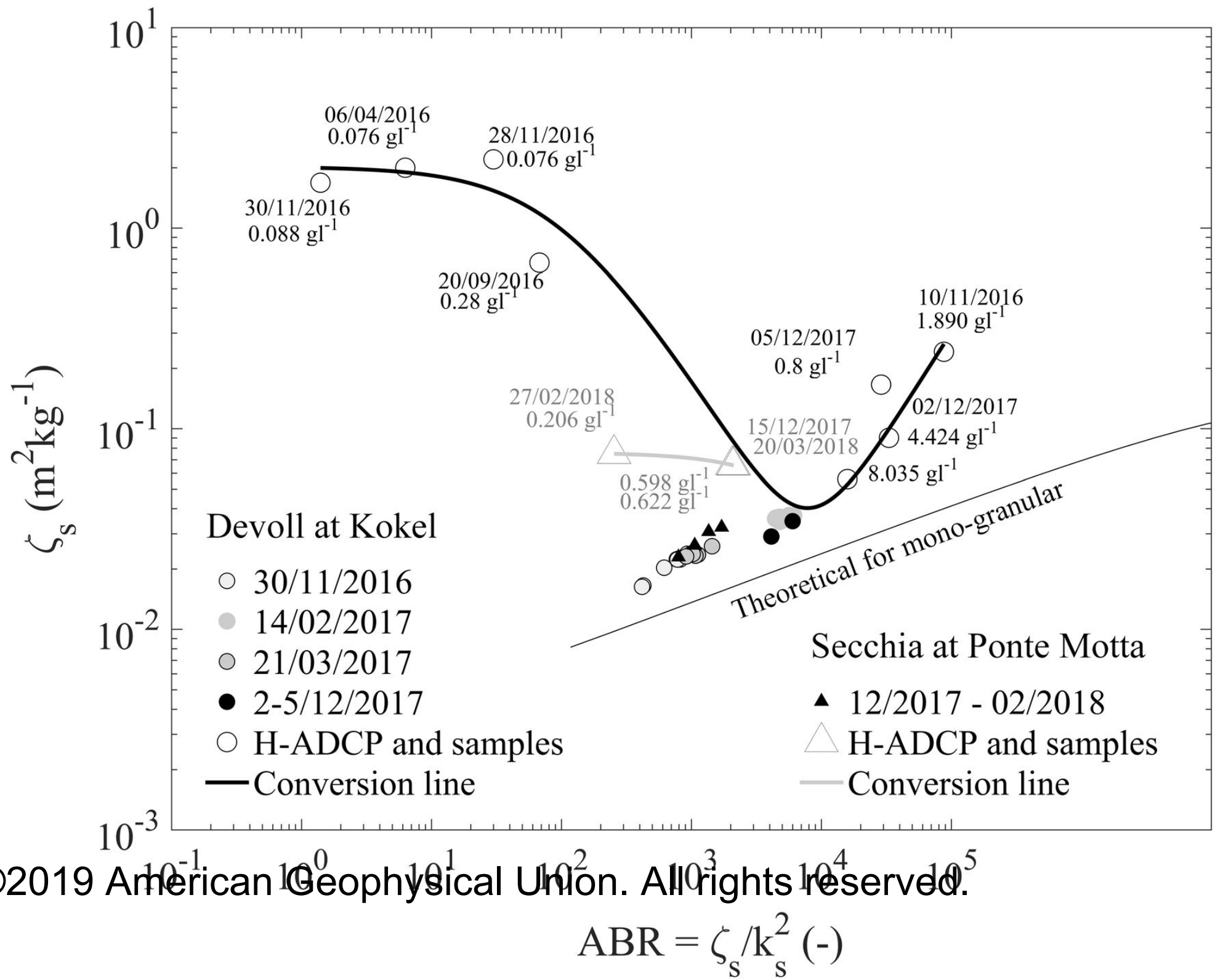

Figure 7 Comparison between acoustically inferred SSC and corresponding values from samples. The improvement of the proposed ABR-method with respect to the attenuation method which doesn't account for.

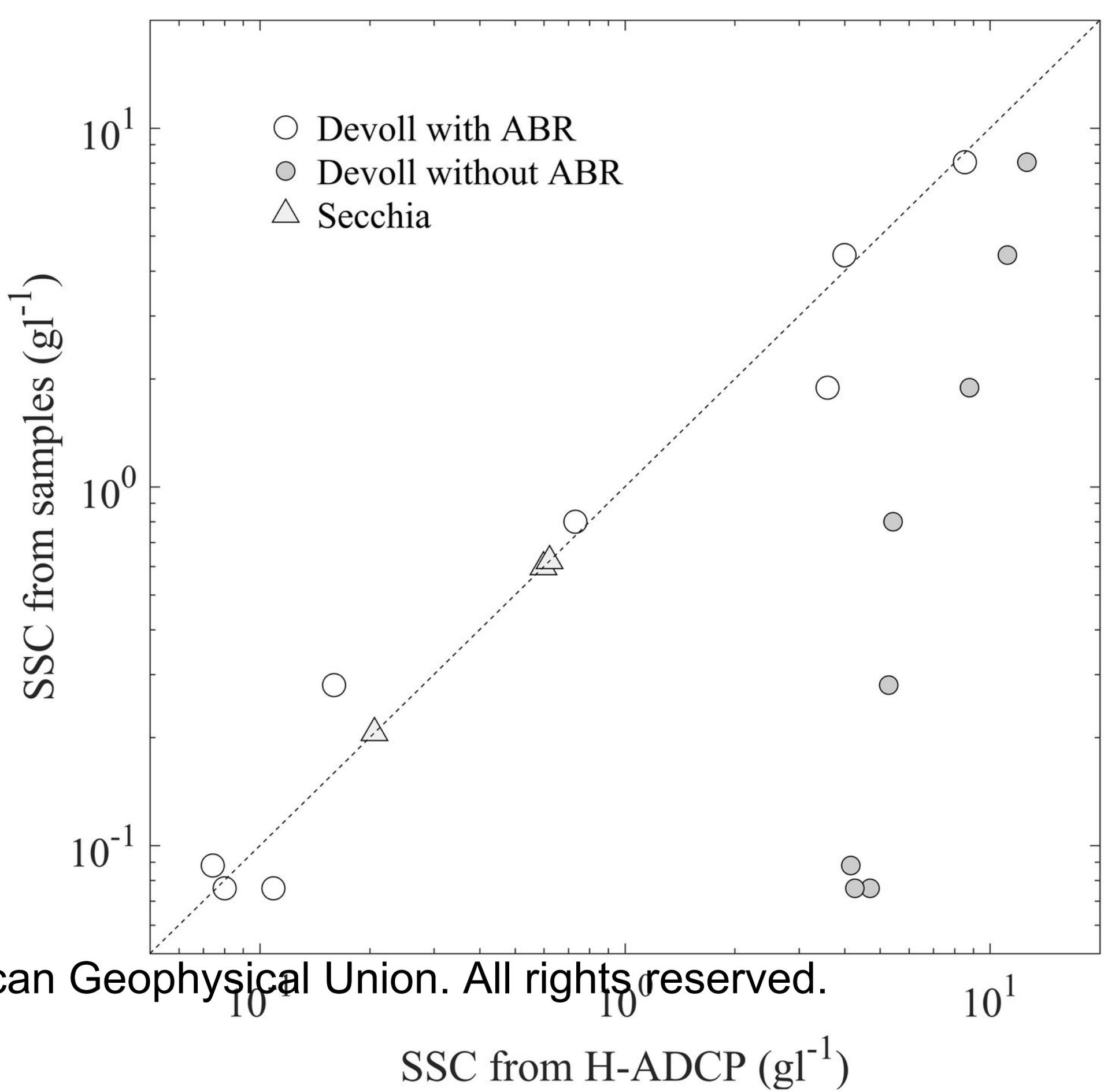

Figure 8 Time series of flow rate, Q, and SSC, C, for rivers (a) Secchia and (b) Devoll for the months November and December 2017..

(a)

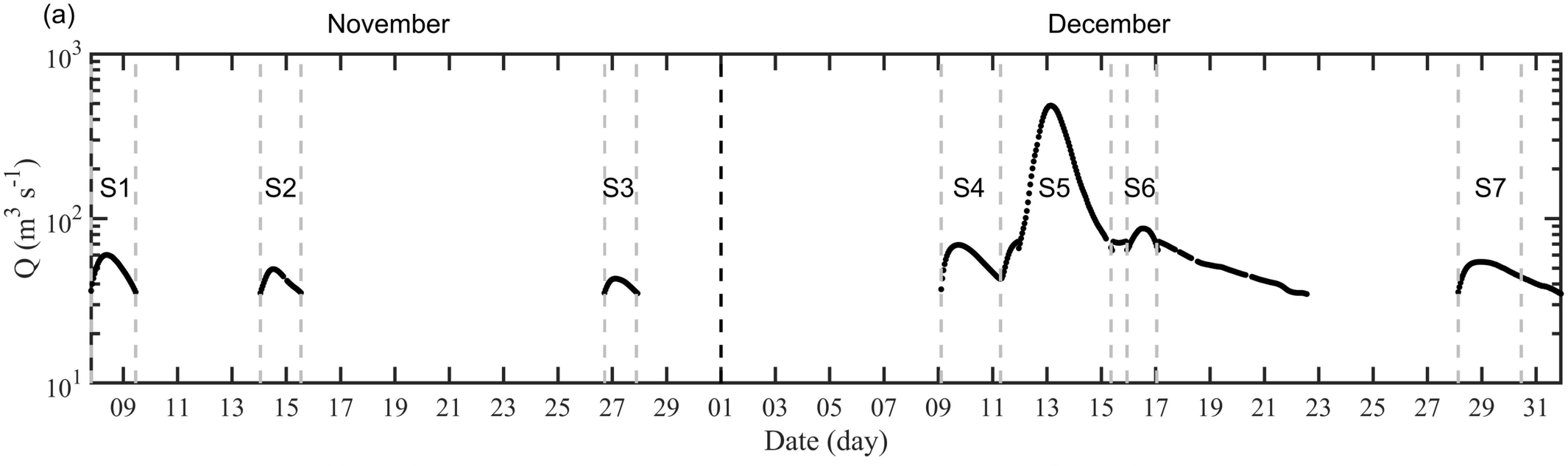

(b)

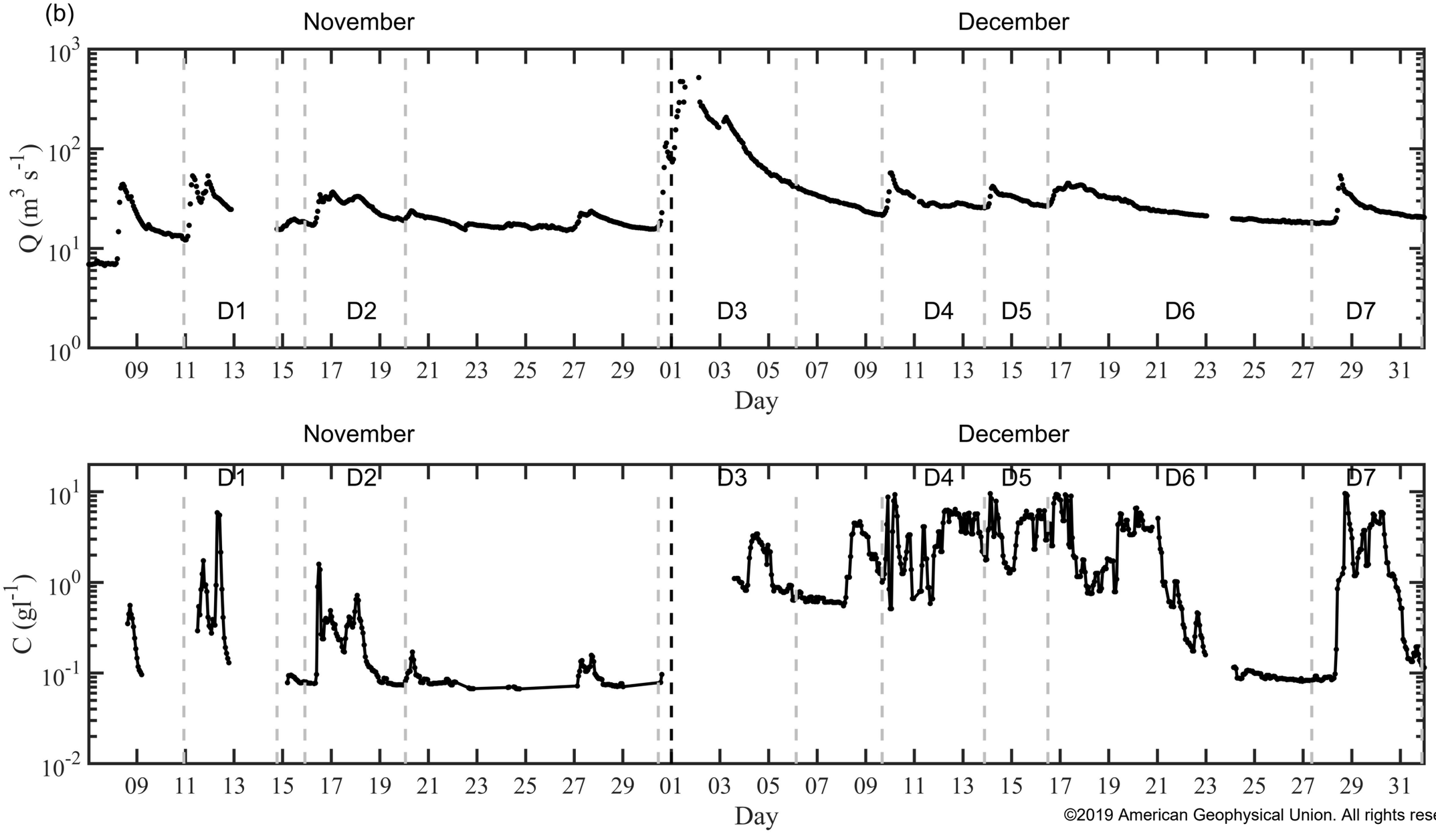

Figure 9 Flow rate (Q) versus SSC (C) distributions for (a) Secchia River and (b) Devoll River. Data is coloured as a function of the ABR..

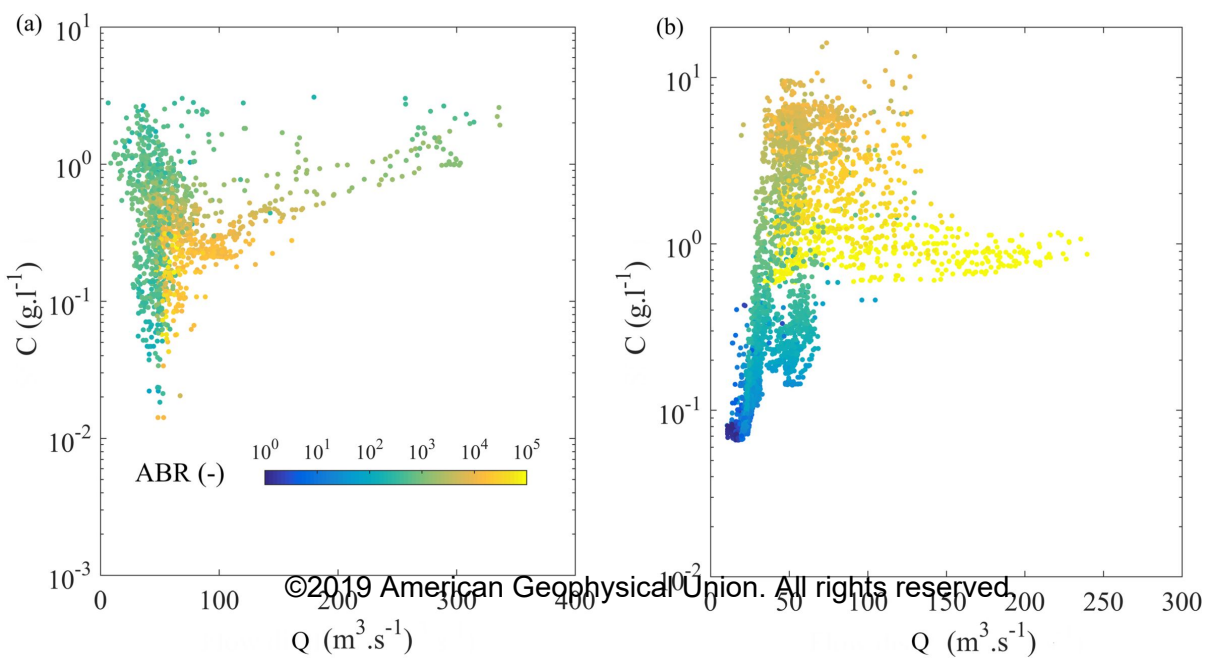

Figure 10 Analysis of three events for rivers (a) Secchia and (b) Devoll. Black triangle denotes the start of the event and the circle the end of the event..

(a)

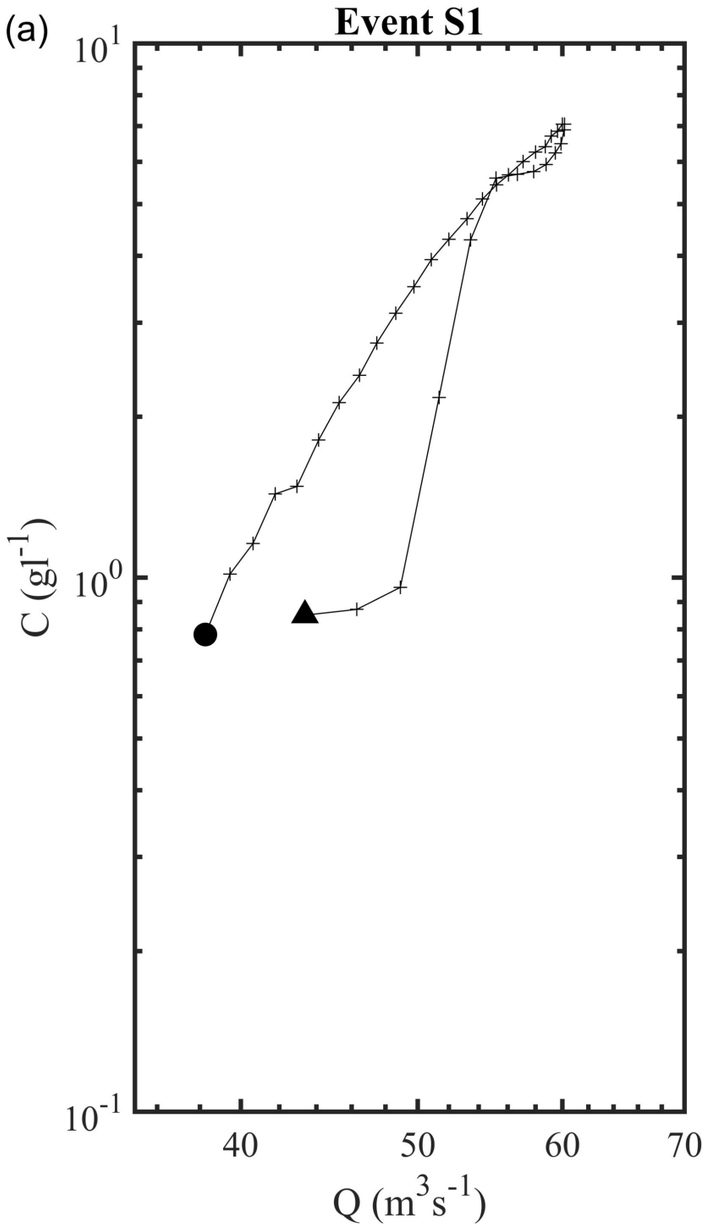

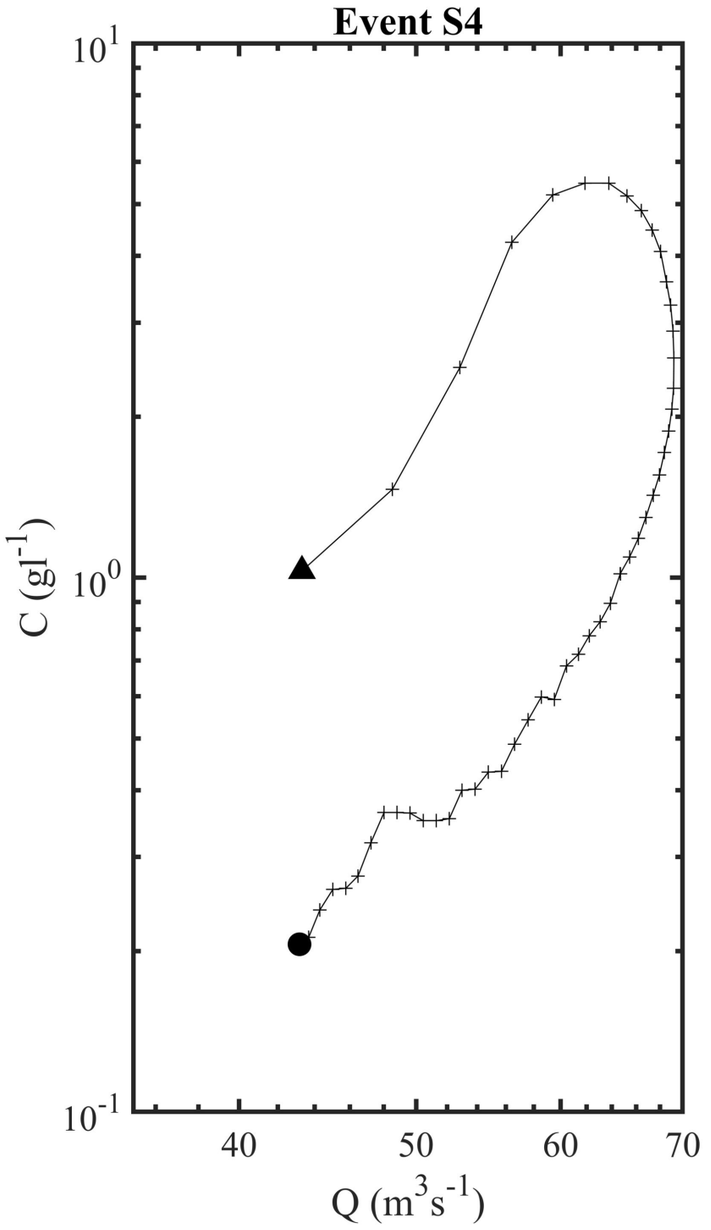

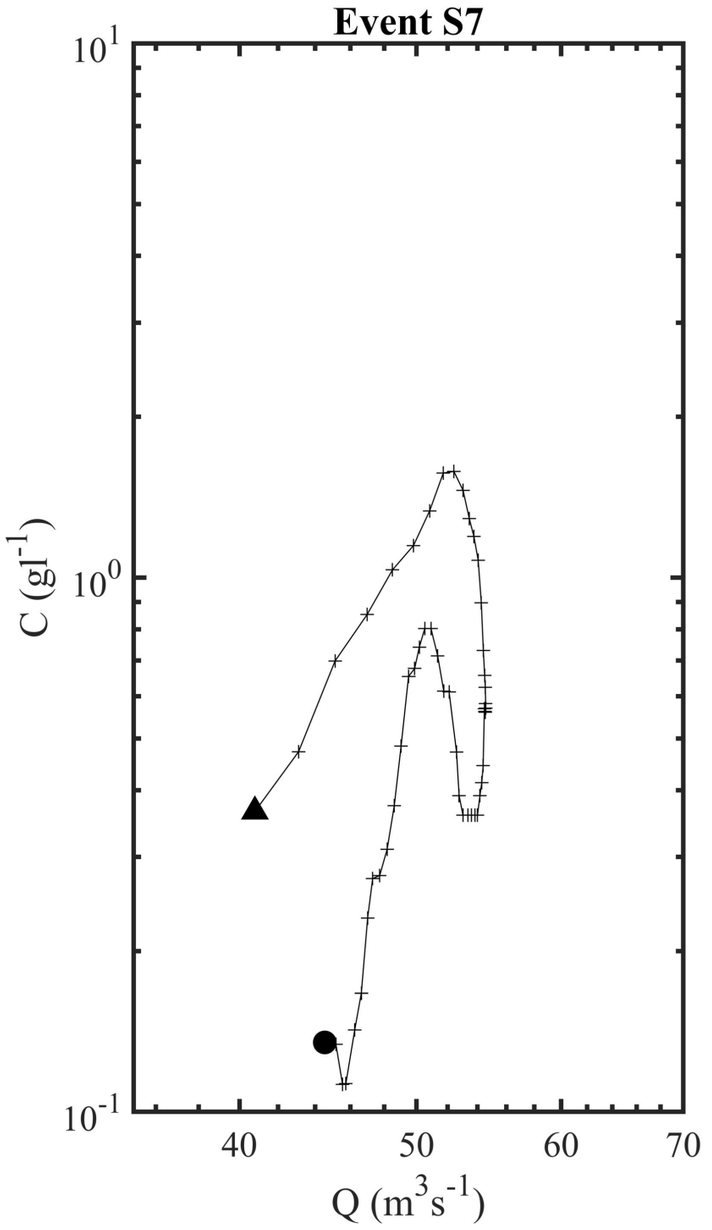

(b)